European Gravity Service for Improved Emergency Management (EGSIEM)—from concept to implementation

Adrian Jäggi,[1] M. Weigelt,[2] F. Flechtner,[3,4] A. Güntner,[4] T. Mayer-Gürr,[5] S. Martinis,[6] S. Bruinsma,[7] J. Flury,[2] S. Bourgogne,[8] H. Steffen,[9] U. Meyer [ID],[1] Y. Jean,[1] A. Sušnik,[1,12] A. Grahsl,[1] D. Arnold,[1] K. Cann-Guthauser,[1] R. Dach,[1] Z. Li,[10] Q. Chen,[10] T. van Dam,[10] C. Gruber [ID],[4] L. Poropat,[4] B. Gouweleeuw,[4] A. Kvas [ID],[5] B. Klinger,[5] J.-M. Lemoine,[7] R. Biancale,[7] H. Zwenzner,[6] T. Bandikova[11] and A. Shabanloui[2]

[1] *Astronomical Institute, University of Bern, Sidlerstrasse 5, CH-3012 Bern, Switzerland. E-mail: adrian.jaeggi@aiub.unibe.ch*
[2] *Institut für Erdmessung, University of Hannover, Schneiderberg 50, 30167 Hannover, Germany*
[3] *Department of Geodesy and Geoinformation Science, Technische Universität Berlin, Strasse des 17. Juni 135, 10623 Berlin, Germany*
[4] *German Research Centre for Geosciences, Telegrafenberg, 14473 Potsdam, Germany*
[5] *Institute of Geodesy, Technical University of Graz, Steyrergasse 30/III, 8010 Graz, Austria*
[6] *German Remote Sensing Data Center, Deutsches Zentrum für Luft-und Raumfahrt, Münchener Strasse 20, 82234 Wessling, Germany*
[7] *Department of Terrestrial and Planetary Geodesy, Centre National d'Etudes Spatiales, Avenue E. Belin 18, 31401 Toulouse, France*
[8] *Stellar Space Studies, Esplanade Compans Caffarelli, 31071 Toulouse, France*
[9] *Lantmäteriet, Geodetisk Infrastruktur, Lantmäterigatan 2c, 80182 Gävle, Sweden*
[10] *Geophysics Laboratory, University of Luxembourg, Rue Richard Coudenhove-Kalergi, 1359 Luxembourg, Luxembourg*
[11] *NASA, Jet Propulsion Laboratory, 4800 Oak Grove Dr, Passadena, CA 91109, USA*
[12] *Geospatial Engineering, Newcastle University, G.15 Cassie Building, Newcastle NE1 7RU, UK .*

SUMMARY

Earth observation satellites yield a wealth of data for scientific, operational and commercial exploitation. However, the redistribution of mass in the system Earth is not yet part of the standard inventory of Earth Observation (EO) data products to date. It is derived from the Gravity Recovery and Climate Experiment (GRACE) mission and its Follow-On mission (GRACE-FO). Among many other applications, mass redistribution provides fundamental insights into the global water cycle. Changes in continental water storage impact the regional water budget and can, in extreme cases, result in floods and droughts that often claim a high toll on infrastructure, economy and human lives. The initiative for a European Gravity Service for Improved Emergency Management (EGSIEM) established three different prototype services to promote the unique value of mass redistribution products for Earth Observation in general and for early-warning systems in particular. The first prototype service is a scientific combination service to derive improved mass redistribution products from the combined knowledge of the European GRACE analysis centres. Second, the timeliness and reliability of such products is a primary concern for any early-warning system and therefore EGSIEM established a prototype for a near real-time service that provides dedicated gravity field information with a maximum latency of 5 d. Third, EGSIEM established a prototype of a hydrological/early warning service that derives wetness indices as indicators of hydrological extremes and assessed their potential for timely scheduling of high-resolution optical/radar satellites for follow-up observations in case of evolving hydrological extreme events.

Key words: Hydrology; Global change from geodesy; Satellite gravity; Time variable gravity.

1 INTRODUCTION

Until the end of the last century, global monitoring of temporal changes in the distribution of environmental mass had been a challenge. Before the advent of satellite missions dedicated to global gravity field recovery such as the CHAllenging Minisatellite Payload (CHAMP; *cf.* Reigber *et al.* 1998), the Gravity Recovery and Climate Experiment (GRACE; *cf.* Tapley *et al.* 2004), and the

Gravity field and steady-state Ocean Circulation Explorer (GOCE; *cf.* Drinkwater *et al.* 2006), geodetic satellites tracked by Satellite Laser Ranging (SLR) and altimeter and other satellites tracked by Doppler Orbitography and Radiopositioning Integrated by Satellite (DORIS) made the biggest contribution to the determination of Earth's gravity field models (e.g. Cheng *et al.* 1997; Lemoine *et al.* 1997; Bianco *et al.* 1998). However, since the launch of the dedicated GRACE mission in 2002, intersatellite ranging has been established as the state-of-the-art technique to globally observe mass variations in the system Earth from space, as evidenced by several thousand scientific publications in the meantime. Although GRACE enabled spectacular science results, for example, summarized by Wouters *et al.* (2014) and Tapley *et al.* (2019), numerous important questions regarding the changes and dynamic processes in the continental hydrology, cryosphere, ocean, atmosphere and solid Earth remain unresolved (Pail *et al.* 2015). Sustained and improved observation systems such as the recently launched GRACE Follow-On (GRACE-FO; Flechtner *et al.* 2013) and next generation gravity missions (e.g. Cesare *et al.* 2013) are needed to extend the available time-series and to provide another leap in accuracy and spatial resolution. This will be a prerequisite to, for example, better separate human-induced changes from natural climate changes. However, a full exploitation of the potential of future gravity missions will only be possible if this may also be achieved for the less precise data of the current GRACE mission and if, in parallel, limiting error sources such as accelerometer errors and temporal aliasing errors may be further reduced (Loomis *et al.* 2012; Flechtner *et al.* 2016).

More than 17 yr after the launch of the GRACE satellites, the exploitation of the GRACE data is still ongoing. A growing number of Analysis Centres (ACs) inside and outside the GRACE Science Data System (SDS) is still challenged with the Level-1B data processing. To date each new release of monthly gravity fields, provided to the scientific user community as Level-2 products in a (usually) spherical harmonic (SH) representation, still represents a substantial and significant improvement with respect to previous releases. Official SDS solutions are provided by the Center for Space Research (CSR; Bettadpur 2012) and the German Research Center for Geosciences (GFZ; Dahle *et al.* 2012). Additional solutions are computed by the Jet Propulsion Laboratory (JPL) for validation (Watkins & Yuan 2012). Apart from these official monthly GRACE gravity field solutions, a growing number of ACs are providing additional solutions, for example, the Centre National d'Etudes Spatiales (CNES; Bruinsma *et al.* 2010), the Technical University of Graz (TUG, solutions labelled ITSG Mayer-Gürr *et al.* 2010) and the Astronomical Institute of the University of Bern (AIUB; Meyer *et al.* 2016). Unfortunately, however, the release of different ACs are not in every case fully comparable. This is mainly observed in terms of noise (Jean *et al.* 2018), but sometimes differences may also result in terms of signal due to different processing strategies. A well-known pitfall was the GFZ RL05 solution (Dahle *et al.* 2014) as illustrated in Fig. 1 for Greenland mass change estimates. At the end of the shown time period substantial differences of a few hundred Gigatons have been observed with respect to the other solutions due to an unintended (hidden) regularization, which was caused by separating the inherently linked orbit determination of the two GRACE satellites from the process of recovering the gravity field (Meyer *et al.* 2015). As a lesson learned one may conclude that a certain agreement on common processing standards will help to ensure the compatibility of the different solutions in view of a proper geophysical interpretation.

On the other hand, the example of the GFZ RL05 solution also nicely shows that the availability of several competing solutions is

very beneficial to detect outliers. The current situation is, however, sub-optimal from the user perspective to fully exploit the information content offered by the data of the past GRACE and the recently launched GRACE-FO mission. Today the end user is essentially left with the difficult choice of deciding (1) which solutions from which AC to use and (2) what actions to perform for converting SH coefficients (Level-2 products) into gridded mass values (Level-3 products) appropriate for their study when not selecting one of the three official SDS solutions.[1]

In contrast to other Earth Observation (EO) data, satellite-based measurements of gravity represent total water storage variations, that is, variations of all surface and subsurface water storage compartments. As such the past GRACE and the recently launched GRACE-FO mission provide unique information on the wetness state of a river basin with regard to its actual flood generation potential or its susceptibility to a drought. Reager & Famiglietti (2009) estimated flood potential at the regional scale by means of determining repeated maxima in water storage anomalies, which suggest an effective storage capacity in a region, beyond which additional precipitation must be met by increases in runoff or evaporation. Thomas *et al.* (2014) presented a quantitative approach for measuring hydrological drought occurrence and severity based on GRACE data by calculating the magnitude of the deviation of regional, monthly total water storage anomalies from the time-series' monthly climatology. Humphrey *et al.* (2016) surveyed key features of temporal variability in the GRACE record by decomposing gridded times-series of monthly equivalent water height (EWH) into linear trends, interannual, seasonal and intra-annual components, with an additional focus on extreme dry anomalies and their relation to documented drought events.

Today it takes approximately two months from the time that the Level-1B data is collected onboard the GRACE satellites to the time when scientists can access and examine the Level-2 or Level-3 products provided to the scientific community. The temporal sampling of the gravity field solutions is at best 10 d but most reliably restricted to one month when not using regularization techniques (Bruinsma *et al.* 2010). Both of these time constraints currently limit the potential of using the results from satellite gravimetry in time-critical monitoring applications (Pail *et al.* 2015). This applies in particular for early-warning and forecasting systems of extreme hydrological events. Flood forecast models need, for example, near real-time (NRT) information to estimate the probable development of the event in terms of flood stage or river discharge with typical lead times of a few days for larger river basins (see overview by Emerton *et al.* 2016). Also the usefulness of high-resolution follow-up observations such as optical and radar EO data for emergency management is strongly influenced by the time-span from alert reception, satellite programming, satellite acquisition and data reception (Voigt *et al.* 2016).

Given these limitations, the GRACE ACs in Europe have joined forces and established the European Gravity Service for Improved Emergency Management (EGSIEM) project, an initiative supported by the Horizon 2020 Framework Program for Research and Innovation of the European Commission and the Swiss State Secretariat for Education, Research and Innovation (SERI). In this article the EGSIEM concept is presented, the current implementation status is reported and future perspectives are outlined. The article is structured as follows: Section 2 introduces the general concept

[1]The US Tellus website http://grace.jpl.nasa.gov/data/monthly-mass-grids is only dedicated to monthly gravity field models of the GRACE SDS ACs
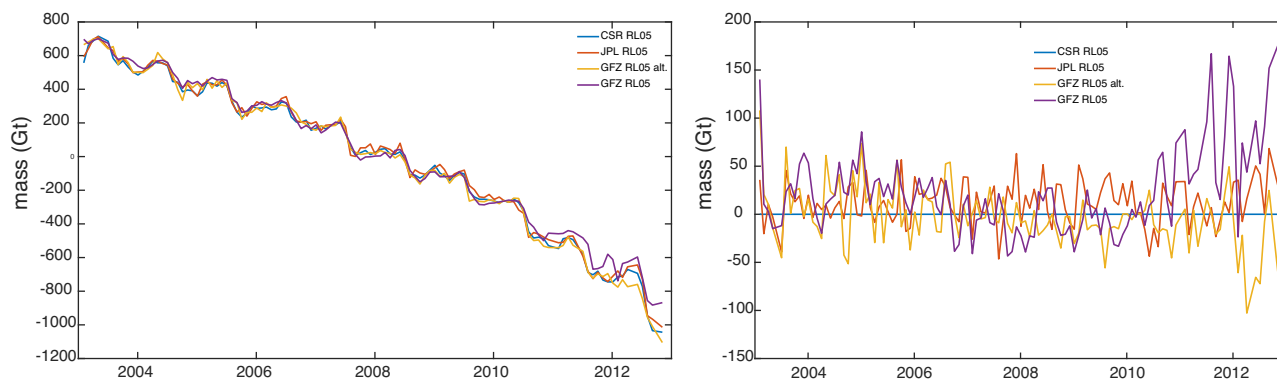
Figure 1. Trends of Greenland mass change estimated from different releases of SDS solutions (RL05) based on different processing strategies (left-hand panel) and with respect to the CSR solution (right-hand panel). No filtering and no further corrections (GIA, leakage) are applied.

of the EGSIEM initiative. Section 3 presents the complementary data prepared within EGSIEM, whereas Section 3.2 is dedicated to the GRACE Level-1B data processing. Sections 4–6 introduce the EGSIEM prototype services and present the current achievements. Section 7 closes the article with a summary and outlook.

2 CONCEPT OF EGSIEM AND ITS PROTOTYPE SERVICES

The main driver of the EGSIEM initiative was that gravity-based observations of the redistribution of water and ice masses provide valuable and complementary information with respect to more traditional EO data as provided by, for example, Copernicus, the European Programme for the establishment of a European capacity for Earth Observation.[2] We, therefore, defined three key objectives: (1) demonstrating that superior gravity products can be derived by combining solutions from different ACs, (2) providing NRT gravity products and (3) assessing the potential of these NRT products for flood and drought monitoring and forecasting. These objectives are achieved by setting up three dedicated prototype services, namely a scientific combination service, a NRT service and a hydrological service. Fig. 2 illustrates the EGSIEM service structure, the interaction between the individual services and the input data used. The services and the achieved results are described in more detail in Sections 4, 5 and 6, respectively.

2.1 Scientific combination service

The main input data to the first two EGSIEM prototype services are GRACE Level-1B data. For combination purposes, Level-1B data needs to be consistently processed by several ACs in the post-processing mode to derive monthly gravity field solutions. These are then combined by the Scientific Combination Service to derive high quality scientific products with a time resolution of one month and latencies of up to 60 d. Since all EO systems must refer to one and the same reference frame, the consistent use of the reference frame is an essential step in the EGSIEM concept. To the extent possible a generic formulation of processing standards has been developed and consequently been applied for the GRACE processing at all EGSIEM ACs (EGSIEM 2015). It is expected that the measures pave the way for a long awaited standardization in the gravity field

community and to significantly increase the quality, robustness and reliability of products derived from satellite gravimetry.

A dedicated GPS reprocessing campaign was conducted for a consistent integration of data from the global tracking network of the International GNSS Service (IGS; *cf.* Dow *et al.* 2009) as described in Section 3.1 and to provide one single set of up-to-date GPS products to all EGSIEM ACs (see Section 3.1). Subsequently, ACs may then apply their preferred, individual approach to process the GRACE input data. The approaches differ by the used observables, the parametrizations, the stochastic noise models applied and the relative weighting of the different observables. All ACs are *required* to provide free solutions, that is, solutions that do not depend on an *a priori* gravity model. This is of crucial importance to avoid biases in the combined solutions. If all solutions are unbiased, the strengths and weaknesses as well as the different background models of the different solutions are expected to average out in the combination and the combined solution will be statistically better and more robust. Details about the processing strategies and the specific background models used at the individual EGSIEM ACs are documented in EGSIEM (2015).

2.2 Near real-time service

The main input data are again GRACE Level-1B data for the recovery of the Earth's gravity field but this time individual ACs derive in their NRT mode rapid gravity products for flood and drought alerting with latencies down to 5 d. The increased temporal resolution from typically 1 month to 1 d is achieved by using sophisticated regularization techniques to compensate for the loss of spatial resolution.

GFZ converts the measured intersatellite tracking data by means of spacecraft velocities into daily differences of the dynamic forcing acting on the twin satellites that are then reduced by forces stemming from geophysical background models and non-conservative origin. The reduced data are then projected by means of functions of geopotential gradient differences to Earth gravity potential variations at ground level. The TU Graz approach directly relates the measured kinematic orbit positions and intersatellite tracking data to the unknown gravity field parameters. After reduction of all modelled forces, the daily gravity variations are recovered using the methodology of Kurtenbach *et al.* (2012). Further details are provided in Section 5.

The provision of the corresponding NRT gravity field information within 5 d is a unique product that has the potential to translate into added value for warning and forecasting the onset of natural hazards.
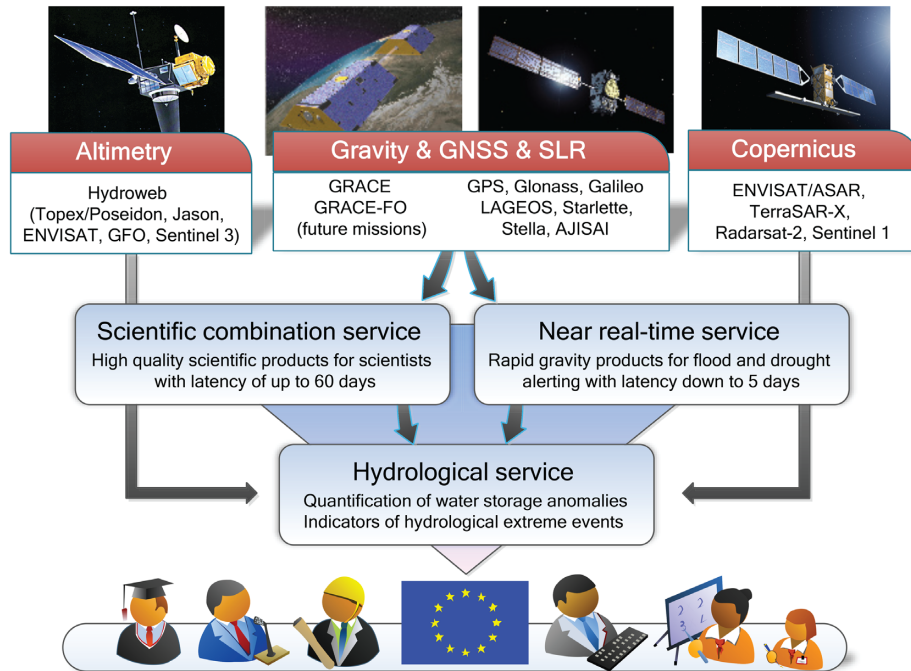
[2]http://www.copernicus.eu

Figure 2. General concept of the EGSIEM: Satellite data from Altimetry, Gravity, GNSS, SLR and Copernicus missions were used to create three prototype services.

2.3 Hydrological service

The main input data of the Hydrological Service are the rapid gravity products from the NRT service to quantify water storage anomalies and to derive indicators of hydrological extreme events such as floods and droughts, whereas the post-processed combined monthly solutions are used for comparison purposes. Their value is especially assessed in view of supporting operational satellite-based flood information services such as those within the framework of the DLR's (Deutsches Zentrum für Luft-und Raumfahrt) Center for Satellite Based Crisis Information (ZKI[3]). A large variety of other EO data such as medium- to high-resolution Synthetic Aperture Radar (SAR) and optical satellite data, for example, from Envisat ASAR, TerraSAR-X, MODIS, Sentinel-1 and the Laboratoire d'Etudes en Géophysique et Océanographie Spatiales (LEGOS) hydroweb data base from altimetry as well as global flood data bases such as the Dartmouth Flood Observatory (Brakenridge 2016) are analysed to compile suitable historical and large-scale flood situations to assess the value of the gravity-based flood and drought indicators.

3 REPROCESSING OF INPUT DATA

3.1 GNSS reprocessing

Besides ultraprecise K-Band intersatellite ranging, the GRACE satellites, as well as all other dedicated gravity missions, are equipped with onboard dual-frequency Global Positioning System (GPS) receivers to allow for precise GPS high-low satellite-to-satellite tracking (GPS hl-SST). In case of the GRACE and the recently launched GRACE-FO mission the analysis of GPS data is thus an inherent part of the Level-1B data processing to

infer monthly gravity field solutions (e.g. Beutler *et al.* 2010). For this purpose high-quality information on GPS satellite orbits and GPS satellite clock corrections is necessary. State-of-the-art products are routinely provided by the International GNSS Service (IGS; *cf.* Dow *et al.* 2009). The operational IGS products are, however, continuously improved by taking the latest developments into account, for example, updates in the underlying reference frame (Altamimi *et al.* 2011, 2016) or the conventions recommended by the International Earth Rotation and Reference Systems Service (IERS; *cf.* Petit & Luzum 2010). As a consequence the operational products are inevitably inhomogeneous over time. Reprocessing campaigns are thus needed to serve applications where long and homogenously processed GPS product series are crucial (e.g. Steigenberger *et al.* 2006; Fritsche *et al.* 2014).

Because previous IGS reprocessings did not usually provide the necessary high-rate (5 s) GPS satellite clock information, as it is needed for a most precise determination of the orbits of low Earth orbiting (LEO) satellites (Bock *et al.* 2009), a dedicated reprocessing effort was initiated within the frame of EGSIEM (Sušnik *et al.*, in preparation). This allowed us to take into account the latest improvements in GNSS orbit modelling (Arnold *et al.* 2015), which in turn allowed for a further improvement in kinematic LEO orbit determination and the subsequent recovery of the Earth's gravity field from kinematic positions. For the first time 5 s high-rate satellite clock corrections are not only provided for the GPS but also for the GLONASS satellites. This reprocessing campaign thus not only assisted spaceborne GPS but also terrestrial multi-GNSS precise point position (PPP) applications (Zumberge *et al.* 1997). GLONASS satellite clock corrections are provided after the year 2008 (30 s) when the full GLONASS constellation was complete, and with 5 s sampling from 2010 onwards. For a detailed description of the EGSIEM reprocessing campaign we refer to Sušnik *et al.* (in preparation).

---

[3]http://www.zki.dlr.de

3.2 GRACE reprocessing

Each associated AC was requested to provide monthly gravity fields of 2006-2007 that agreed with the EGSIEM standards concerning reference frame, Earth orientation, satellite geometry/antenna reference points, relativistic effects and third bodies perturbing the satellites' motion. The processing had to be based on common GPS orbits and clock corrections (see Section 3.1). All gravity field contributions were requested to be free solutions (i.e. not regularized) complete to degree and order 90. The normal equations of the monthly GRACE gravity fields were generated in the Solution (Software/technique) INdependent EXchange (SINEX) format.

This reprocessing was used by the individual analysis centres to revise their processing strategy in general. Major changes compared to the pre-EGSIEM gravity field time-series were

(1) AIUB: revision of observation screening, low-pass filtering of geometric K-band correction,

(2) GFZ: 3 hr accelerometer scale factors and biases in three directions, down-weighting of GPS phase observations from 0.7 to 1.0 cm mean error, ocean tide model update to FES2014 (Carrere *et al.* 2016),

(3) CNES: free and complete solution instead of single-value-decomposition (SVD) approach, extension to degree and order 90, revision of relative weighting GPS/KRR, reduction of resolution of GPS-contribution to degree and order 40.

(4) TUG: introduction of observation screening, use of star camera and accelerometer sensor fusion attitude data and geometric K-band correction, accelerometer parametrization (e.g. full scale matrix; see Klinger *et al.* 2016), orbit integration based on elliptic reference orbit instead of linear motion, increase of correlation length of empirical covariances from 1 to 3 hr, improved constraining of co-estimated daily variations based on geophysical models.

In Fig. 3 we compare the EGSIEM releases of the individual gravity fields with their respective predecessors for the 2 yr demonstration period of 2006-07. It illustrates global grids of the RMS of EWH anomalies. Anomalies are defined by subtraction of deterministic models of secular and seasonal changes per grid cell from monthly grids of EWH variations. While over the continents strong non-seasonal signals of mainly hydological origin are visible, the ocean areas are very quiet, with few exceptions like in the South Atlantic. We therefore concentrate on the oceans to assess the noise content of the gravity field time-series. A significant reduction of noise is visible in the case of TUG and GFZ, a minor reduction of noise in the case of AIUB. For CNES no corresponding comparison can be shown since no free solution comparable to the EGSIEM release exists.

4 SCIENTIFIC COMBINATION SERVICE

The goals of the scientific combination service as described in Section 2 are achieved by careful standardization, screening and combination of the individual AC solutions described in Section 3.2. Relative weights are derived on solution level by variance component estimation. The final combination is performed on normal equation level to produce optimally combined solutions. Eventually external validations are investigated to independently assess the quality of the derived solutions.

4.1 Combination approach

To ensure the quality of the combined products, the individual contributions are compared in terms of signal and noise content. The signal content is assessed by analysing the amplitude of seasonal variations of EWH in three selected river basins and by ice mass trends in Greenland and West Antarctica (e.g. Meyer *et al.* 2016). An attempt to characterize the noise levels is made by the evaluation of anomalies, that is, the monthly variability after subtraction of a deterministic model of secular and seasonal variations. Anomalies are studied either spatially in regions of little variability, that is, over the oceans, or spectrally for a range of spherical harmonic coefficients with a strong noise contribution, for example, between about degrees 50–90. The purpose of the comparison is twofold. Time-series of monthly gravity fields with reduced signal content, for example, due to regularization, are rejected in order to avoid a bias in the combined solution. Furthermore, individual monthly gravity fields with increased noise level, for example, due to bad observational data, are also screened out in order to not deteriorate the combined solution.

4.1.1 Level-2 products

After individual screening all ACs use a subset of the same GRACE K-Band range-rate observations. No additional information is therefore introduced by the combination. But the noise levels of the individual ACs' monthly gravity fields are today still dominated by background model errors (Flechtner *et al.* 2016) and individual analysis noise (Jean *et al.* 2018), but not due to observation errors (see baseline accuracy in Kim 2000). These errors are specific to the individual ACs and therefore reduced in the combination, which in turn increases the signal to noise ratio. In the frame of EGSIEM combinations are performed on both the solution level and the normal equation (NEQ) level. As opposed to the findings of Sakumura *et al.* (2014), who could not demonstrate weighting to be beneficial when combining the three official SDS solutions, a weighted average was found to be crucial to account for the very different noise levels of the individual gravity field solutions. As described in detail by Jean *et al.* (2018), relative weights are iteratively derived per solution for each month by comparing the individual solutions to a weighted average by using the mathematical framework of variance component estimation (e.g. Koch 2007).

The combination on NEQ-level is superior in taking into account the correlations between the estimated corrections to the gravity field model and satellite- and arc-specific instrument and orbit parameters. But due to very diverse noise models and formal error characteristics, a standard weighting scheme based on variance factors (e.g. Koch 2007) does not lead to satisfactory results. To reduce the effect of the different noise models the individual NEQs are scaled until equal contribution of the individual NEQs to pairwise combinations is achieved and consequently the noise-based relative weights derived on solution level are applied as described in detail by Meyer *et al.* (2018).

Within the frame of the EGSIEM project monthly combined solutions were produced for the demonstration period 2006 January to 2007 December. The individual as well as the combined solutions for 2006 January are shown in Fig. 4 in terms of the median (2006-07) of degree amplitudes of anomalies of spherical harmonic coefficients, expressed in EWH. In order to limit the comparison to the physically meaningful part of the spectrum, Fig. 4 (bottom) only considers the orders 0–29. Fig. 4 confirms that the quality of the four individual contributions of the EGSIEM
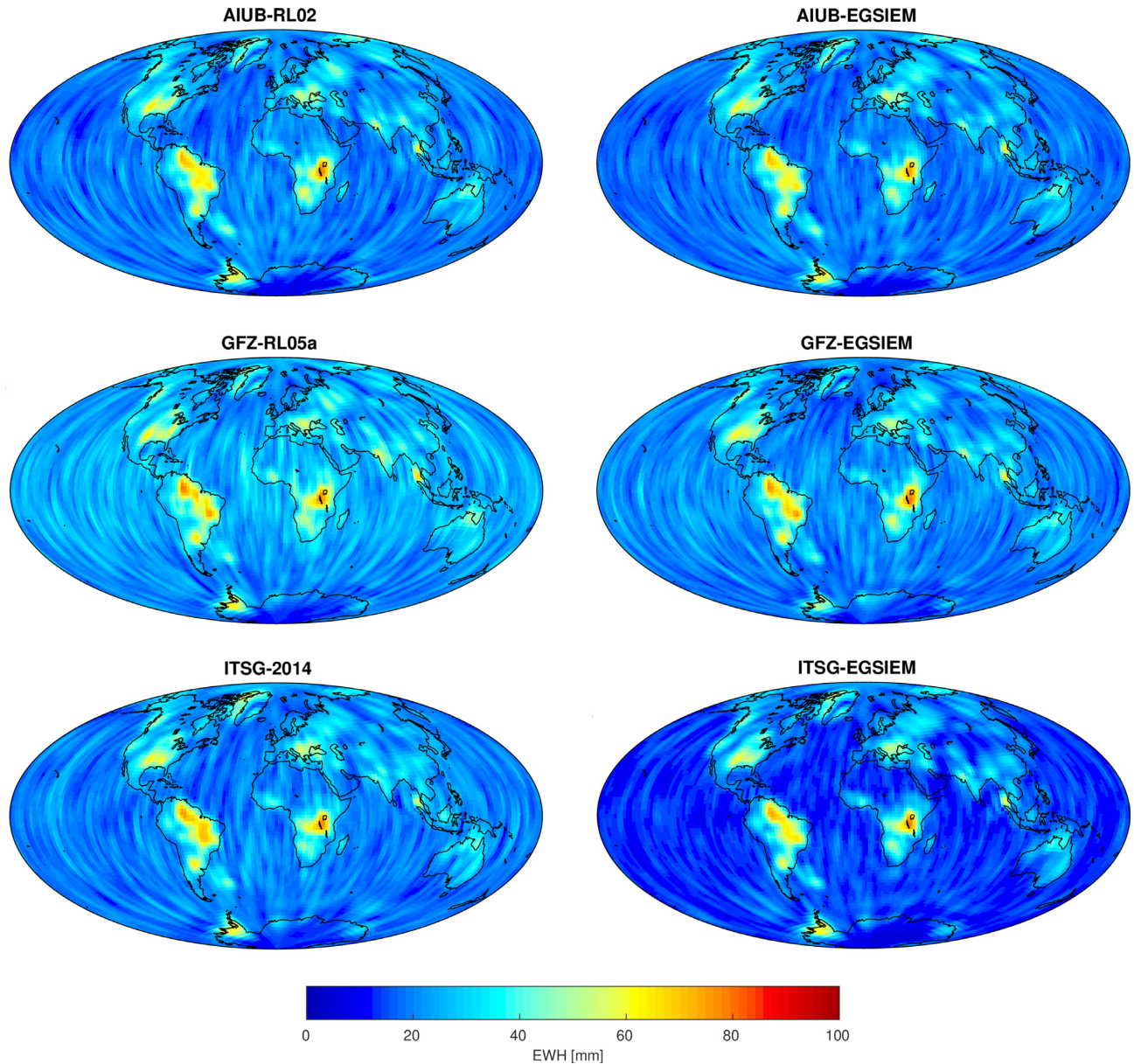
Figure 3. RMS of anomalies of the filtered predecessor releases (left-hand column) and the EGSIEM releases (right-hand column) of the monthly gravity field solutions computed at the different ACs.

ACs is quite diverse, with the ITSG contribution being dominate in terms of low noise. This can be attributed to the different approaches to absorb noise, either by pseudo-stochastic accelerations (AIUB), K-band and accelerometer instrument parameters (GFZ and GRGS) or a sophisticated empirical noise model and observation-dependent weighting (as in case of ITSG). In Fig. 5. the monthly RMS of anomalies over the oceans are shown to assess the noise of the individual and combined solutions in the spatial domain.

The combined solutions outperform the individual contributions in the part of the spectrum with a strong noise component, that is, beyond degree 31 (corresponding to the second resonant order 31). Compared to the combination on solution level, the combination on NEQ-level turns out to be more robust, for example, in the vicinity

of resonant orders, because accuracy information and correlations are taken correctly into account. A more in-depth analysis may be found in Meyer *et al.* (2018).

The combined products may be visualized by the dedicated EGSIEM plotter and are distributed via the EGSIEM webpage[4] and the International Center for Global Earth Models (ICGEM), either in spherical harmonic coefficients (Level-2 products) or as post-processed grids of EWHs (Level-3 products). The latter are generated individually for hydrological and oceanographic applications.
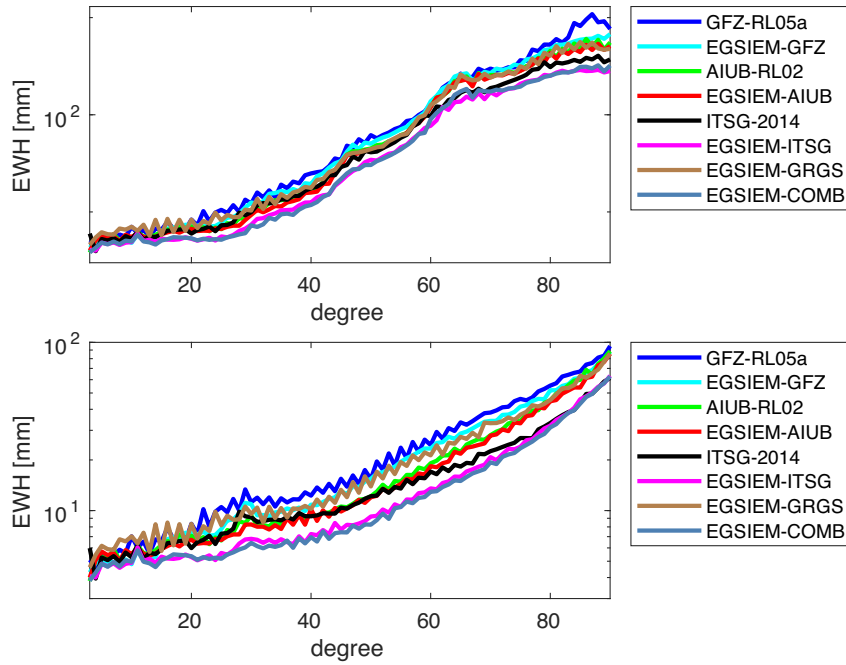
[4]http://www.egsiem.eu

Figure 4. Median (2006–07) of degree amplitudes of coefficient wise anomalies taking into account all orders (top) or only orders up to 29 (bottom).
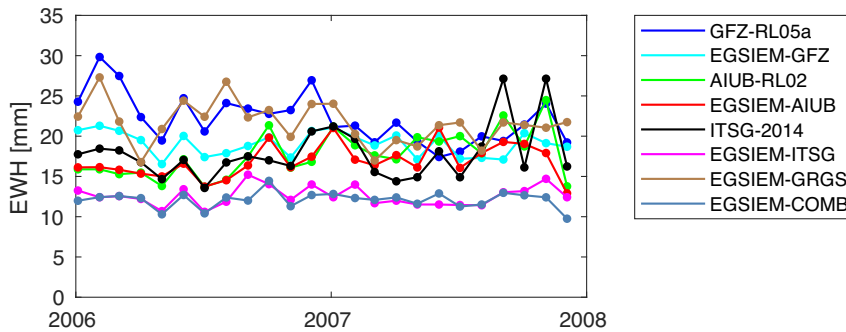

Figure 5. Weighted RMS over the oceans of filtered monthly solutions of the EGSIEM ACs and of the combined monthly solutions.

4.1.2 Level-3 products

To derive Level-3 (Table 1.) from Level-2 products, as a first step the full (non-tidal) signal content is reconstructed by adding the monthly means of the atmosphere and ocean de-alising products back to the monthly fields. These are combined from the monthly means provided by the individual ACs using the same relative weights as derived for the monthly fields by VCE on solution level. As a next step, spherical harmonic degree 1 coefficients derived by Satellite Laser Ranging (SLR) are added to transform from a centre of mass to the centre of figure frame. C_{20} is not replaced, because no clear advantage of SLR derived values over the combined GRACE solution could be found.

The gravity signal induced by the last glaciation about 20 000 yr ago overlaps signals of other sources such as hydrology, and thus needs to be effectively removed with a model of glacial isostatic adjustment (GIA). Within EGSIEM a new GIA model has been developed based on a series of regional ice history models (Tarasov *et al.* 2012; Briggs *et al.* 2014; Lambeck *et al.* 2014; Lecavalier *et al.* 2014; Hughes *et al.* 2015; Nordman *et al.* 2015; Root *et al.* 2015) which were combined temporally and spatially to form a global ice model called LM17.3 (Steffen *et al.* 2017), and the laterally

Table 1. Definition of L3-products.

L3-product	Constituents
GRACE non-tidal	GRACE + monthly means of atmosphere and ocean de-aliasing products
Hydrology	GRACE non-tidal − atmosphere − ocean − GIA
Oceanography	GRACE non-tidal − atmosphere − ocean − GIA − hydrology + OBP

homogeneous VM5a Earth model (Argus *et al.* 2014). The ice model has a spatial resolution of 0.5×0.5 degrees and consists of 52 time steps of different length related to distinct past changes. The GIA model filtered with DDK5 (Kusche *et al.* 2009), called EGSIEM GIA LM17.3 DDK5, can be downloaded from the EGSIEM plotter. It is planned to provide an update with a slightly improved ice model and a laterally heterogeneous (3D) Earth model soon.

For ocean-related applications the monthly mean of ocean bottom pressure (OBP) is added back and a hydrological model is subtracted to avoid signal leakage from the continents (the specific models applied are listed in Table 2). Finally the spherical harmonic coef-

Table 2. Models applied for the definition of Level-3.

Degree 1 SHC	AIUB-SLR[a] (Sośnica *et al.* 2015)
Atmosphere	AOD1B-RL05: GAA
Ocean	AOD1B-RL05: GAB
OBP	AOD1B-RL05: GAD
GIA	LM17.3 (Steffen *et al.* 2017)
Hydrosphere	WGHM, evaluated at the epochs of the monthly GRACE gravity fields (Döll *et al.* 2003)

[a]ftp://ftp.unibe.ch/aiub/GRAVITY/SLR/SLR_degree_1.txt

ficients are transformed to global grids with one degree resolution, applying specific filters for either hydrological or oceanographic applications. The filter matrices are derived in analogy to the DDK filters (Kusche *et al.* 2009), but instead of a simulated, average GRACE noise model, the monthly calibrated errors of EGSIEM-ITSG are used. All monthly filter matrices are available to the users via the EGSIEM webpage.

4.2 External validation of gravity field solutions

Ensuring data quality is an essential part of EGSIEM. This is achieved by comparing gravity-field derived station displacements with vertical displacement time-series derived from GNSS according to Davis *et al.* (2004) and van Dam *et al.* (2007). Besides the individual solutions derived by the four individual ACs in Section 3.2 and the EGSIEM combined solution from Section 4.1, we additionally include also the three SDS gravity field solutions. Note that we have validated all the EGSIEM Level-2 and Level-3 gravity products within the EGSIEM project, while we present here only results of validating Level-2 combined gravity solutions. For results of validating other EGSIEM gravity products, readers are referred to Chen *et al.* (2018).

The validation procedure described here closely follows Chen *et al.* (2018). This includes post-processing of the GRACE data, processing of three different GNSS data sets used for the validation, as well as the computation of performance evaluation indicators, which are degree and cumulative degree WRMS reduction measures. For detailed information regarding these aspects we refer to Chen *et al.* (2018). Here we only mention some slight differences with respect to Chen *et al.* (2018). For the GRACE data post-processing we add back SLR-derived degree 1 coefficients from Sośnica *et al.* (2015) and we restore the AOD1B atmospheric and oceanic dealiasing products from the EGSIEM combined dealiasing products (see Section 4.1). Regarding the three GNSS station time-series, we use only those station time-series that do not suffer from any data gap within the 2-yr period of our EGSIEM gravity field solutions. As such, we have 178 station coordinates from the EGSIEM GNSS reprocessing products (see Section 3.1), (2) coordinate solutions of 388 stations from the ITRF2014 realization (Rebischung *et al.* 2016) and (3) 377 station time-series of the JPL GNSS products (Bock *et al.* 2012).

Fig. 6 shows the mean degree WRMS reductions and mean cumulative degree WRMS reductions of the eight different gravity field solutions in comparison to the ITRF2014 displacements, which demonstrates similar characteristics as in Chen *et al.* (2018) in terms of degree contributions. In the context of this article, we are primarily interested in the relative performance of the various solutions. Both the mean degree WRMS and especially the mean cumulative degree WRMS reduction indicate that the combined EGSIEM solutions generally provide the strongest WRMS reductions. Also two of the individual AC solutions, AIUB and ITSG, outperform

the three SDS solutions in the low degrees, which can be assigned to the consequent implementation of the processing standards to ensure a higher consistency with the IGS processing standards. Nevertheless, it has to be noted that the ACs solutions from GFZ and GRGS currently do not provide good results at certain low degrees, in particular the imperfect performance at degree 2. Via the degree WRMS reduction analysis, we are able to track the degree 2 problem of the EGSIEM-GRGS solution down to be caused by C_{21} and S_{21} terms. Further investigation will be needed to identify the reason of this abnormal behaviour. It is interesting to note that the combined solutions were able to overcome the degree 2 problems from the EGSIEM-GRGS solution and perform best among all EGSIEM solutions, which confirms once more the hypothesis that the combination of solutions may yield an improvement in the gravity field solutions.

Fig. 7 shows in the spatial domain the WRMS of the reduction at the 388 GNSS stations of the two time-series, that is, one gravity field solution and the ITRF2014 station displacements. Visually, yellow to red colours dominate the spatial patterns indicating strong agreements between GNSS and GRACE. Up to 72.13 per cent of WRMS reduction is observed using the EGSIEM-COMB solution at CUIB located in Cuiabá, Brazil and similar patterns are also seen for other gravity solutions. The negative WRMS reductions (light blue to black dots) mostly appear in the GNSS stations located in islands or along the coast which are possibly affected by non-tidal oceanic effects (Tesmer *et al.* 2011) or even spurious long-period signals due to unmodelled short-periodic displacements (Penna *et al.* 2007).

To be more specific, a summary of statistics is displayed in Table 3 which shows the mean and median WRMS reductions on the full signal level as well as the annual signal level from eight gravity solutions with respect to the three GNSS products. With respect to the ITRF2014 and EGSIEM-reprocessed GNSS time-series, the EGSIEM combined solution provides the best statistic numbers in terms of both the full signal and the annual signal level. For instance, up to 26.65 per cent mean WRMS reduction at the full signal level is observed for the EGSIEM-COMB solution comparing to the EGSIEM-reprocessed GNSS time-series. In comparison to the JPL GNSS time-series, the EGSIEM-COMB also demonstrates the top performance as the EGSIEM-ITSG and CSR RL05 gravity solutions.

5 NRT-SERVICE

The goal of the NRT-Service was to provide daily gravity field solutions with a latency of maximum 5 d. For this purpose, two independent approaches were developed at the German Research Centre for Geosciences (GFZ) and TU Graz (TUG) based on a Kalman filter approach, first introduced by Kurtenbach *et al.* (2012).

Common to both approaches is the input data consisting of rapid GNSS products provided by the centre of orbit determination (CODE; Dach *et al.* 2009, 2017), JPL's GRACE Level-1B quick-look data and the GFZ Release 6 GRACE Level-1B atmosphere and ocean de-aliasing product (AOD1B RL06; Dobslaw *et al.* 2017) that are both provided within the GRACE Science Data System. These data sets feature a latency of 17, 24 and 10 hr, respectively, which meets the above requirements to produce NRT gravity field solutions. Since data pre-processing, outlier detection and gravity field computation in both approaches differ significantly, two suitably independent solutions are produced on a daily basis.

GFZ converts the measured intersatellite range-rates and range-accelerations by means of spacecraft velocities derived from precise
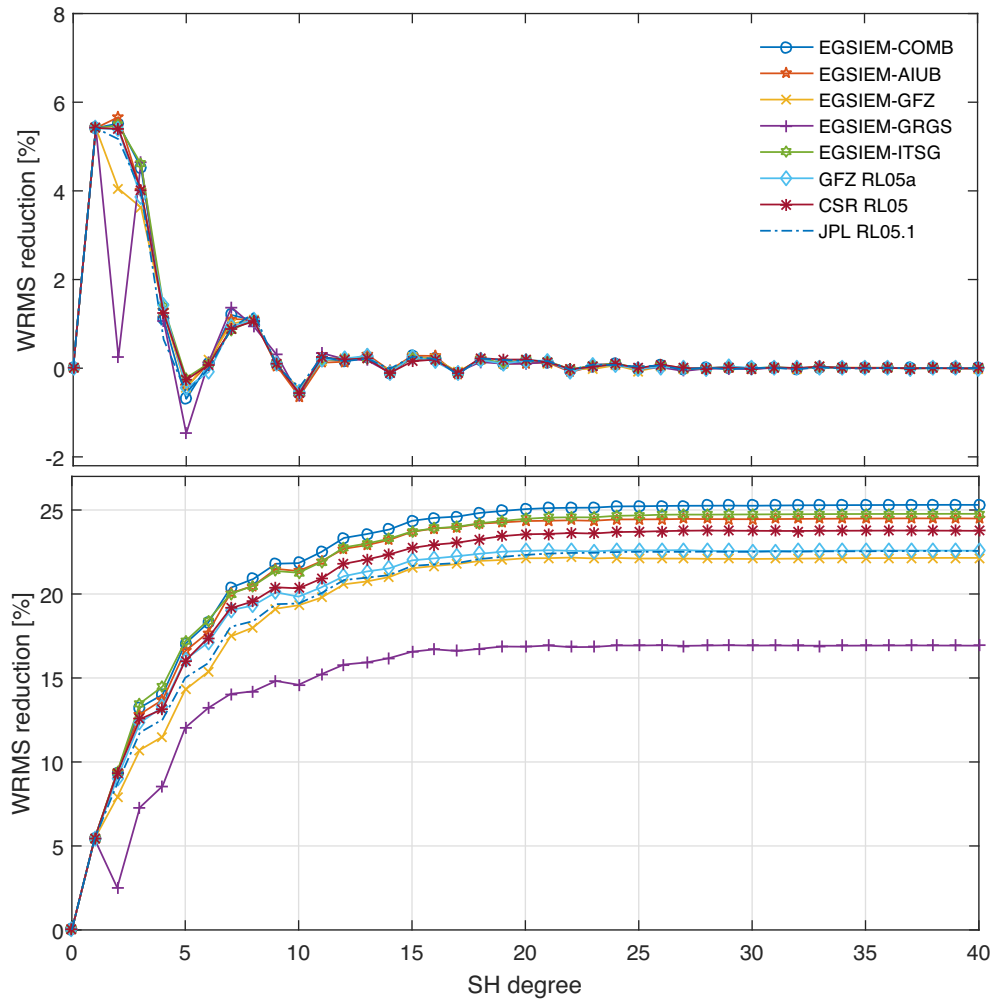
Figure 6. Mean degree WRMS reductions (top) and mean accumulative degree WRMS reductions (bottom) of the eight gravity solutions with respect to the ITRF2014 GNSS residuals on the full signal level at 388 GNSS stations. As no significant contributions come from degrees beyond 30, we truncate the plots at degree 40. EGSIEM-COMB indicates the EGSIEM combined solutions at the NEQ level. EGSIEM-AIUB, EGSIEM-GFZ, EGSIEM-GRGS and EGSIEM-ITSG represent gravity solutions from the four individual ACs.

orbit determination (POD) into differences of the dynamic forcing acting on the twin satellites. These derived dynamic observations can be reduced by forces stemming from geophysical background models, representing the lithosphere density contrast (static gravity field), third body attractions, ocean tides, atmospheric and oceanic non-tidal mass variations (AOD1B) and forces of non-conservative (mainly drag and solar radiation pressure) origin. The reduced data is then projected by means of functions of geopotential gradient differences to Earth gravity potential variations at ground level and expressed in equivalent water layer thickness. The spherical mean Earth surface is discretized into 2×2 arc degree equal area surface tiles that are post-processed to regular 2x2 arc degree grids and can be further decomposed in spherical harmonic coefficients for the generation of additional (e.g. Level-3) products. Daily updates are computed in a Kalman filter approach, where external data sets provide the constraints for a prediction in time, driven by the expected average temporal variation of daily water storage in the hydrological system derived from WGHM (Döll *et al.* 2003) and atmospheric and oceanic mass variations derived from AOD1B. Secular variations, for example, of the cryosphere, are contained in the background gravity field model (EIGEN-6C; Shako *et al.* 2014)

and are therefore reduced from observations beforehand. This results in statistically smooth and stationary signal. Multistep noise estimates for the observed dynamic forcing completes the measurement update in the Kalman filter. The main idea behind this is the whitening of the observation residuals after the surface signal computation step, which is achieved for the respective autocorrelations if they reduce to Dirac-like pulses. A detailed description of the methodology can be found in Gruber & Gouweleeuw (2019).

TUG relies on intersatellite range rate and kinematic orbit positions that are related to the unknown gravity field parameters by means of variational equations. The gravity field is parametrized by a spherical harmonic series up to degree and order 40. The processing of the GRACE Level-1B data closely follows the strategy used for TUG's monthly solutions (Klinger *et al.* 2016; Mayer-Gürr *et al.* 2016; Ellmer *et al.* 2017). A key component of this processing chain is the determination of weighting between the individual observation groups by analysing the post-fit residuals of an unconstrained monthly gravity field solution. Using this weighting, unconstrained daily normal equations, which serve as input for the Kalman filter, are computed. The signal content of these daily normal equations is the residual gravity field left in the GRACE
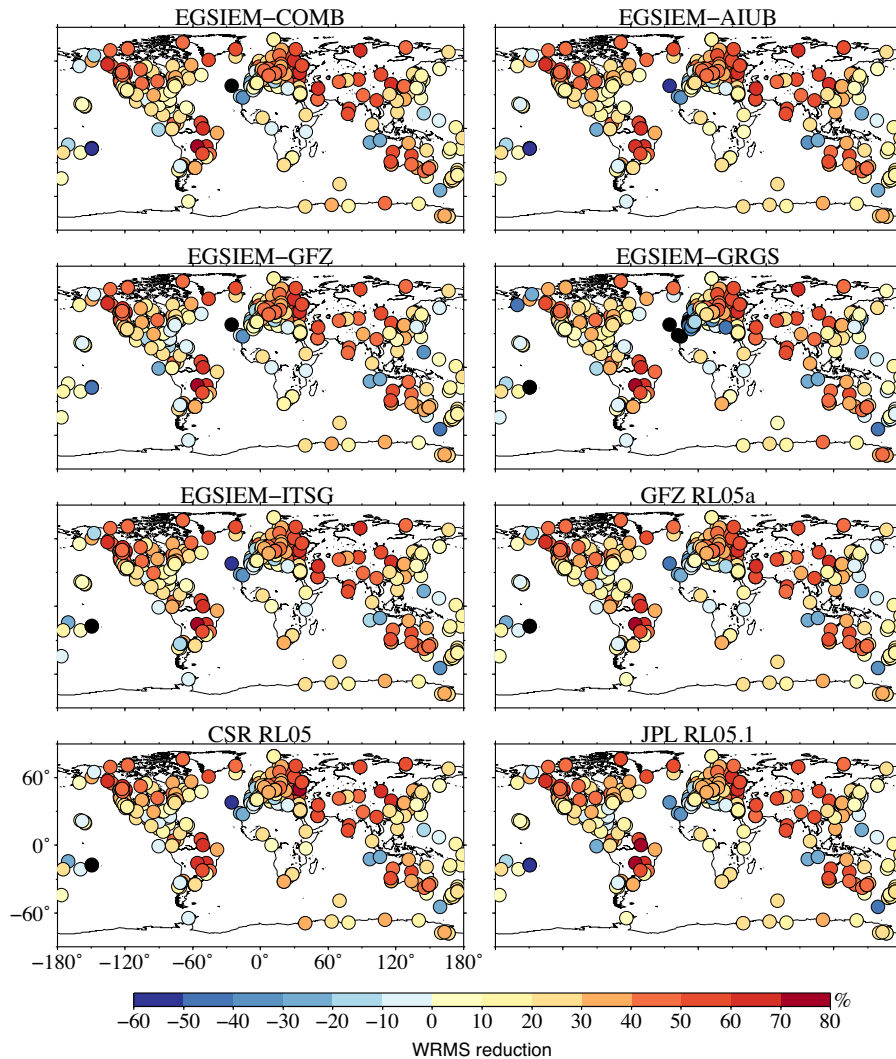
Figure 7. Spatial plots of the WRMS reductions from all the gravity solutions compared to the ITRF2014 GNSS residuals on the full signal level at 388 GNSS stations.

Table 3. Mean WRMS reduction on the full signal level and median WRMS reductions on the annual signal level between eight GRACE gravity products and three GNSS solutions. Best performances are indicated in bold letters.

	ITRF2014		EGSIEM-reprocessed		JPL	
	Full (per cent)	Annual (per cent)	Full (per cent)	Annual (per cent)	Full (per cent)	Annual (per cent)
EGSIEM-COMB	**25.31**	**72.72**	**26.65**	**72.35**	23.59	67.72
EGSIEM-AIUB	24.50	70.64	26.22	70.73	22.81	66.33
EGSIEM-GFZ	22.17	68.28	23.08	67.44	20.27	64.65
EGSIEM-GRGS	16.95	63.64	22.07	66.64	18.41	62.36
EGSIEM-ITSG	24.78	71.63	26.42	69.25	**23.83**	**68.89**
GFZ RL05a	22.61	70.20	24.96	72.01	22.16	65.87
CSR RL05	23.78	70.20	25.94	70.31	23.61	67.75
JPL RL05.1	22.56	69.16	24.41	65.94	21.86	64.14

observations, after reducing all background models. Consequently, the major constituents left are sub-seasonal continental hydrosphere and cryosphere, as well as errors in the dealiasing model. This is reflected in the Kalman filter process dynamics, which is composed of empirical auto- and cross-covariance estimates of geophysical model output of exactly these signal sources. In the case at hand, the hydrosphere is represented by WGHM while cryosphere and

dealiasing errors are represented by the 'I' component and dealiasing model error estimates contained in the ESA Earth System Model (Dobslaw *et al.* 2015). The models were only evaluated up to the beginning of 2002 to avoid any overlap with the GRACE time-series. Furthermore, an isotropic noise component of approximately 7 mm EWH which corresponds to 5 per cent of the average global signal

Table 4. Satellite data acquisitions for the Danube delta in Romania during Charter Call 121.

Satellite	Sensor	Spatial Resolution (m)	Date
SPOT-4	Optical	10	23.04.2006
ERS-2	SAR	30	23.04.2006
Radarsat-1	SAR	30	25.04.2006
ENVISAT-A SAR	SAR	30	28.04.2006

was added to account for unmodelled effects. A detailed description of the methodology may be found in Kvas & Mayer-Gürr (in preparation).

The performance of the daily gravity solutions has been tested using historical hydrological extreme events (Gouweleeuw *et al.* 2018) and relative intercomparisons between both NRT time-series based on global RMS differences (2.53 cm EWH for 2002–2015 and 2.43 cm EWH for 2004–2010) and absolute comparisons with GNSS-derived vertical displacements (2.67 mm for 2002–2015 and 2.51 mm for 2004–2010 in case of TUG; 2.67 and 2.57 mm, respectively, for GFZ). As a threshold the 2002–2015 EWH RMS difference between monthly ITSG-Grace2016 and CSR RL05 solutions is 1.9–2.8 cm depending on the applied filter. The comparison of CSR RL05 with GNSS-derived vertical displacements results in 2.49 mm for 2002–2015 and 2.32 mm for 2004–2010 (Flechtner *et al.* 2017), which demonstrates the excellent performance of both daily time-series.

An operational test run of the NRT service was foreseen in the final phase of the EGSIEM project between 2017 April and September. However, the deteriorating health of GRACE-B posed a serious challenge in GRACE data processing and is the limiting factor in the quality of the gravity field solutions. Following a battery cell failure on 2016 October 25, the accelerometer aboard GRACE-B was turned off. Its data stream has subsequently been replaced with a 'transplant' data product, where the accelerometer measurements of GRACE-A are shifted in time and rotated to substitute the missing measurements on GRACE-B. Furthermore, to shed load on the GRACE batteries following the cell failure, intersatellite K-Band ranging (KBR) data were only collected in orbit segments where the satellites were fully exposed to the sun. Since 2011 the satellites were subject to regular position switching maneuvers to conserve fuel on GRACE-B. These events are correlated with the β angle between the orbit plane and the Earth–Sun direction and have a periodicity of 161 d. When β is smaller than approximately 15°, the intersatellite link was switched off and the KBR data are completely missing.

Following this procedure, intersatellite observations between the GRACE spacecraft were once more available since 2017 March 17. To alleviate the accelerometer transplant process, the pitch angle of both spacecraft relative to the line of sight was increased from zero to approximately one degree (Himanshu Save, Gerhard Kruizinga, personal communication 2017) on March 30 (Fig. 8, left-hand panel). The resulting increased KBR antenna phase centre correction (PCC) magnitude (Fig. 8, right-hand panel) causes errors in spacecraft attitude more prominently propagating into the gravity field solutions and manifest in east-west striping patterns.

KBR data collection was steadily increased from sunlight-only orbital segments (approximately 40 per cent reduction of observation count) to full revolutions. On May 2 the accelerometer on GRACE-B was switched on again for 22 d at the expense of the

amount of KBR data collected during this period. Nevertheless during this time span the nominal set of GRACE science data was available.

The operational phase of the NRT-Service started on April 1 with both GFZ and TUG producing daily GRACE solutions in an automated manner until 2017 June 29, when the instruments have been switched-off again. In fact these were the last gravity measurements of GRACE and the mission was officially declared ended on 2017 October 27.[5]

The problems with KBR antenna PCCs described above impacted the quality of the TUG and GFZ models in a different manner. While GFZ relies fully on JPL's PCCs provided within the Level-1B data records, TUG calculates their own correction using a smoothed attitude product based on a combination of star camera observations with angular accelerations (Klinger *et al.* 2014). This combination acts as a low pass filter and reduces high frequency noise in the derived PCC's compared to the Level-1B data set. The discrepancies between the solutions become obvious when looking at daily total water storage maps (Fig. 9) and derived flood indices (Fig. 10) within the operational test run (e.g. 2017 June 5) and a daily solution at 'normal' satellite conditions (e.g. 2008 June 5). In terms of difference RMS over the continents, TUG and GFZ solutions differ approximately 2.8 cm during the NRT service run, which is an increase of about 30 per cent compared to the same three months time span in 2008. Nevertheless, from the historical data it can be concluded that both, the gravity maps (9, top) and the flood indices (Fig. 10, top), look very similar for 2008 and again demonstrate the quality of the TUG and GFZ solutions. Operational latency of the NRT gravity field solutions at TUG is on average below 1 d from the last data epoch collected to the upload of the final solution. GFZ solutions needed about 1 additional day, but in general the latency is also well below the requirement of 5 d.

6 HYDROLOGICAL SERVICE

In order to evaluate whether the NRT solutions from the previous section may be used as an early warning indicator in flood monitoring and alerting services, an appropriate index is needed. Earlier studies, using monthly GRACE water storage anomalies, defined a flood index relative to an effective storage capacity of a region as inferred from repeated maxima in the GRACE time-series (Reager & Famiglietti 2009), or included GRACE-based storage anomalies in an autoregressive model for predicting flood discharge with lead times of up to several months (Reager *et al.* 2014). The Wetness Index (WI) developed here represents the departure (D) of the GRACE-derived total water storage anomaly (X_{tot}) from the mean seasonal cycle (X_{seas}) after removing the long-term trend (X_{long}). WI is expressed in dimensionless units of standard deviation (S), where S is a measure of the variation of D. X_{tot} is the total daily anomaly of mass, expressed in centimetres of equivalent water thickness, relative to the mean of the daily GRACE record considered here (2002 April–2015 December). X_{tot} can be decomposed as follows:

$$X_{tot} = X_{long} + X_{seas} + X_{res} \qquad (1)$$

and

$$X_{long} = X_{inter} + X_{lin}. \qquad (2)$$

[5]https://www.nasa.gov/press-release/prolific-earth-gravity-satellites-end-science-mission
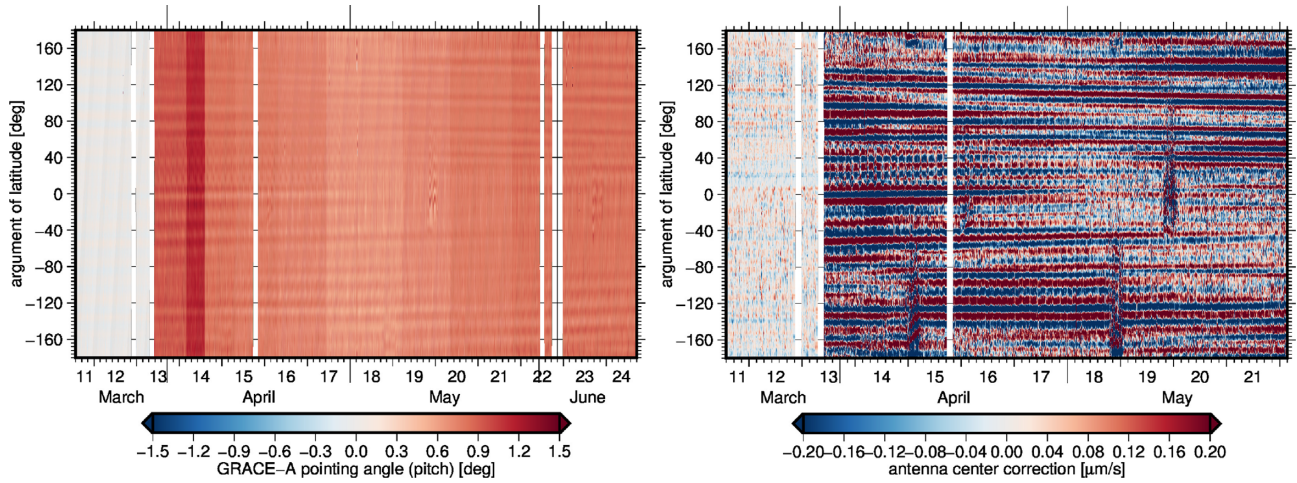
Figure 8. Pointing angle (pitch component) of GRACE-A relative to the line of sight and antenna phase centre corrections (PCC, expressed as range-rate) during the operational NRT service run.
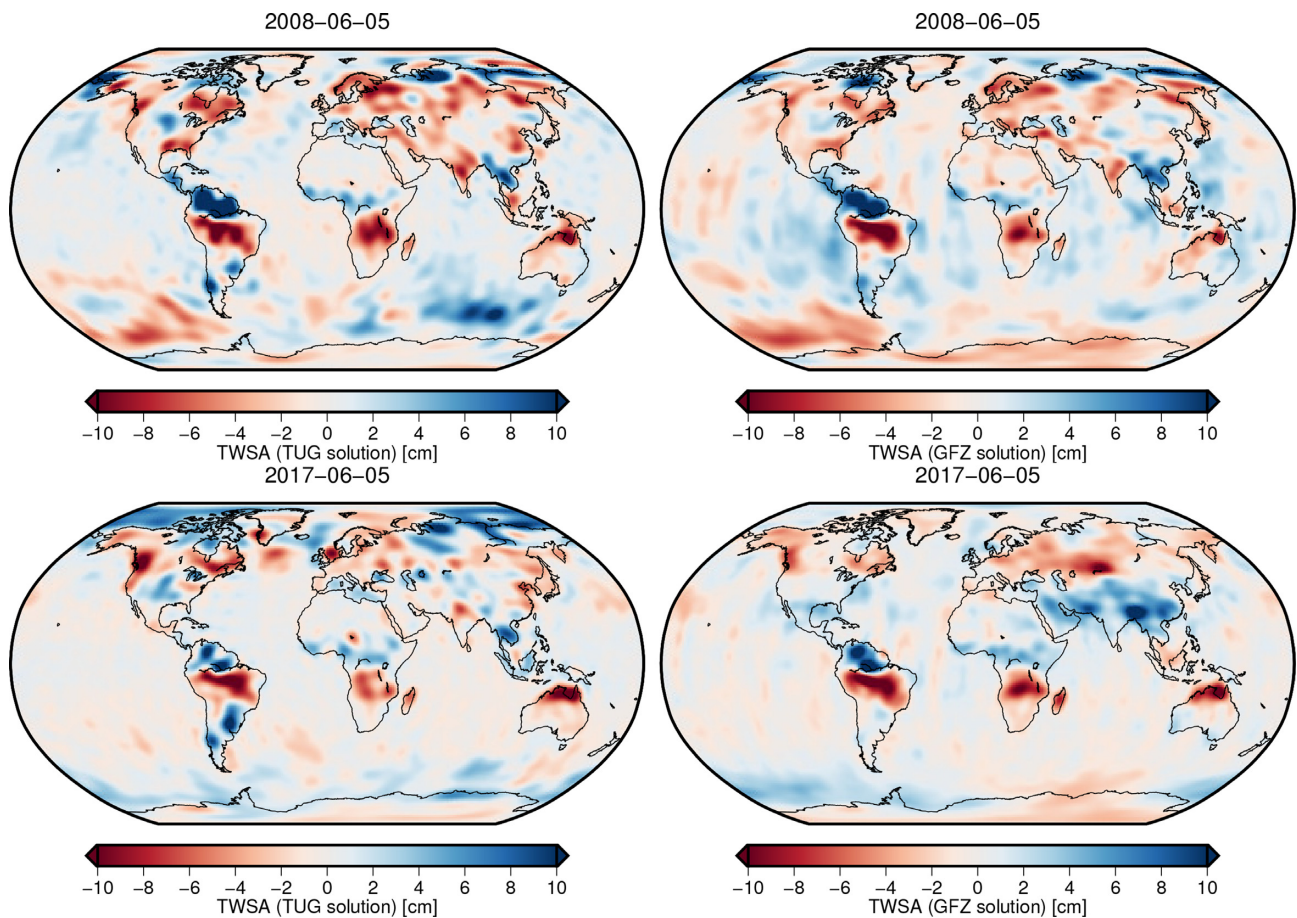

Figure 9. Total water storage anomaly derived from TUG (left-hand panel) and GFZ (right-hand panel) for 2008 June 5 (top) and 2017 June 5 (bottom). A three month mean around the evaluation epoch is subtraced from both time-series.

The long-term component X_{long} is computed by applying a 365 d low-pass filter and, as such, is considered to contain periodicities longer than 12 months only. The interannual variation is calculated as the deviation from the linear trend ($X_{\text{inter}} = X_{\text{long}} - X_{\text{lin}}$). The mean seasonal component is taken as the daily average over the full GRACE record after removing the long-term component. X_{res} is then the residual or irregular component. D is then the sum of the interannual variation X_{inter} and the intra-annual variation or residual X_{res} and expressed as the wetness index WI:

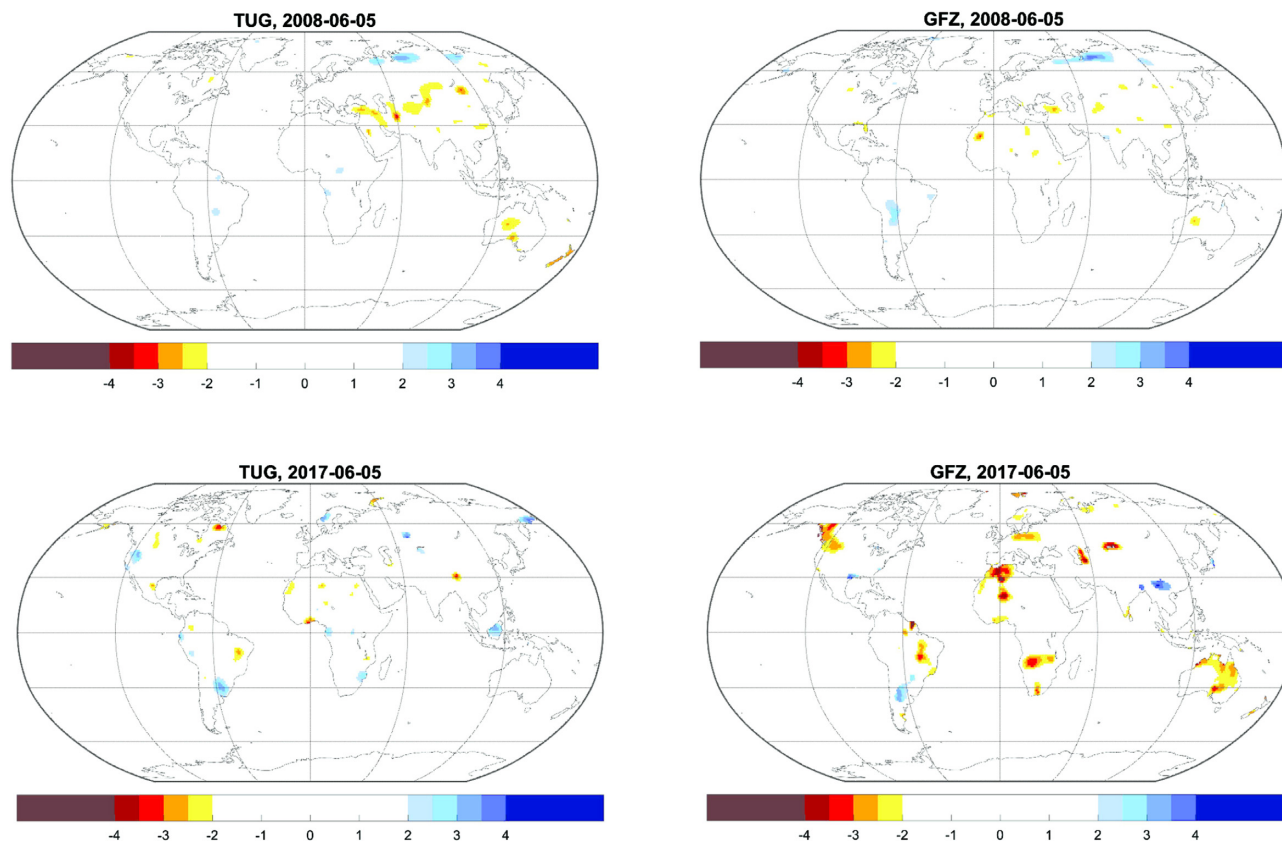$$WI = \frac{D}{S} = \frac{X_{\text{inter}} + X_{\text{res}}}{S}. \tag{3}$$

Figure 10. Wetness indices for TUG (left-hand panel) and GFZ (right-hand panel) NRT gravity products for 2008 June 5 (top) and 2017 June 5 (bottom).

With extreme hydrological events in focus, the most extreme absolute value of either WI on each day is selected for a combined WI.

Fig. 10 shows the above defined WI derived from the TUG and GFZ NRT gravity field solutions presented in Section 5. Similar to the water storage maps in Fig. 9 (top), the geographical patterns of the WI look similar for the two NRT solutions derived from historical data. Fig. 10 (top) shows exceptionally high (Central South America, Siberia) and low (Central Australia, Turkey, Central Asia) values of the wetness index. In contrast, for deficient satellite conditions during the operational NRT test run, the global WI patterns derived from the two solutions considerably differ (Fig. 10, bottom) as also the daily water storage maps differ from each other (Fig. 9, bottom).

6.1 Test case Danube basin

Fig. 11 shows a retrospective analysis of daily global gravity solutions for the years 2002–2015 for the Danube basin. Both the gravity solutions from TUG and GFZ and the WIs derived from these solutions indicate increased values in particular for the flood events in the Danube basin in 2002, 2006 and 2010, and less pronounced for the flood events in 2005, 2009, 2013 and 2014. Particularly relevant with respect to early flood warning is the build-up of basin-wide water storage of several weeks duration prior to the larger flood events of 2006 and 2010, which were triggered by a combination of (early season) snowmelt (resulting from unusual early high temperature peaks in 2006) and intense (2006) or excessive (2010) rainfall (e.g. ICPDR 2007, 2012).

Fig. 12 illustrates the flood and WI dynamics in more detail for the 2006 and 2010 events. River flow at the Ceatal Izmail station at the outlet of the Danube Basin peaks on 2006 April 26. Elevated WI values of about 2, corresponding to the 95 per cent percentile of WI values in the Danube basin, were recorded from early March onwards, possibly indicating a level close to basin storage saturation. A first WI peak over the presumed threshold of 2 on March 14, marked as a (green) vertical line in Fig. 12 (left-hand panel) provides a lead-time to river peak flow at the basin outlet of 43 d (or over 6 weeks). This lead time exceeds the traveltime of flood waves from the upstream to the downstream parts of the basin which is in the order of 3–4 weeks. Fig. 12 (right-hand panel) illustrates the setting for the 2010 Danube flood. River discharge at the basin outlet peaks on July 6. WI values clearly exceeding the indicative threshold of 2 are recorded from May 30 onwards. This leads to a flood warning lead-time prior to peak flow at the basin outlet of 37 d (or over 5 weeks).

A closer look at the figures discussed above reveals different dynamics of the two WIs derived from the individual daily gravity solutions. While the ITSG-derived WI dominates (i.e. generates the more extreme WI values) for the 2006 flood (Fig. 12, left-hand panel), the GFZ-derived WI does so for the 2010 flood (Fig. 12, right-hand panel). This tentatively points to a strength of the combined WI, which selects the most extreme absolute value. Interestingly, in the longer term perspective (2002–2015), the similarity of the two WIs is striking, despite differences in dynamics and/or noise levels of the individual daily gravity solutions they are derived from (Fig. 11c). Here, apart from the larger floods in 2006 and 2010 (exceeding the indicative WI threshold of 2), smaller and shorter duration floods from 2013 and 2014 are detected with shorter lead
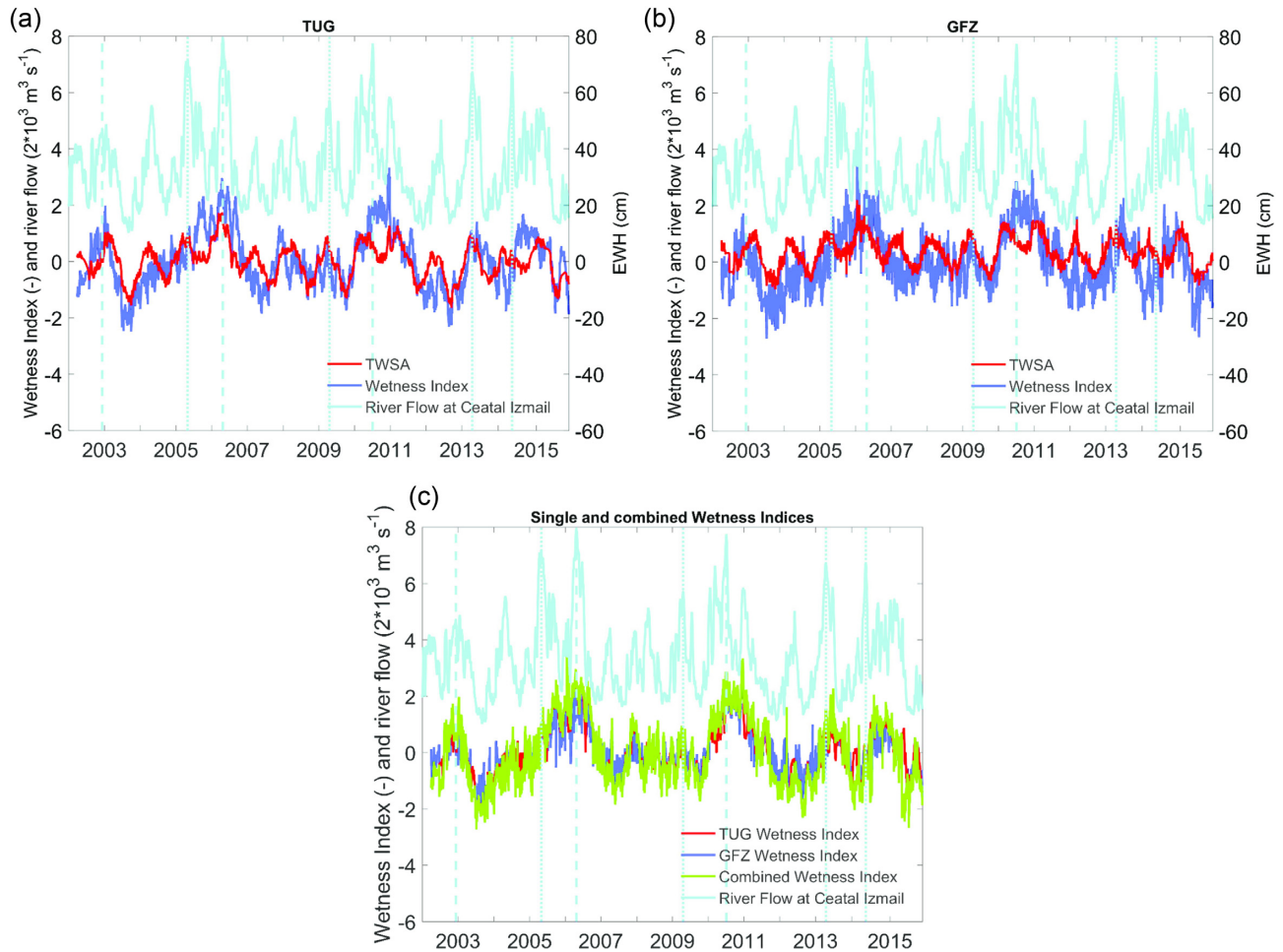
Figure 11. Basin-average daily water storage anomalies (TWSA), gravity-derived WIs and river discharge at Ceatal Izmail gauging station at the basin outlet of the Danube basin (2002–2015) for (a) TUG and (b) GFZ, (c) for the combined WI. The vertical lines indicate the days of peak discharges for flood events.
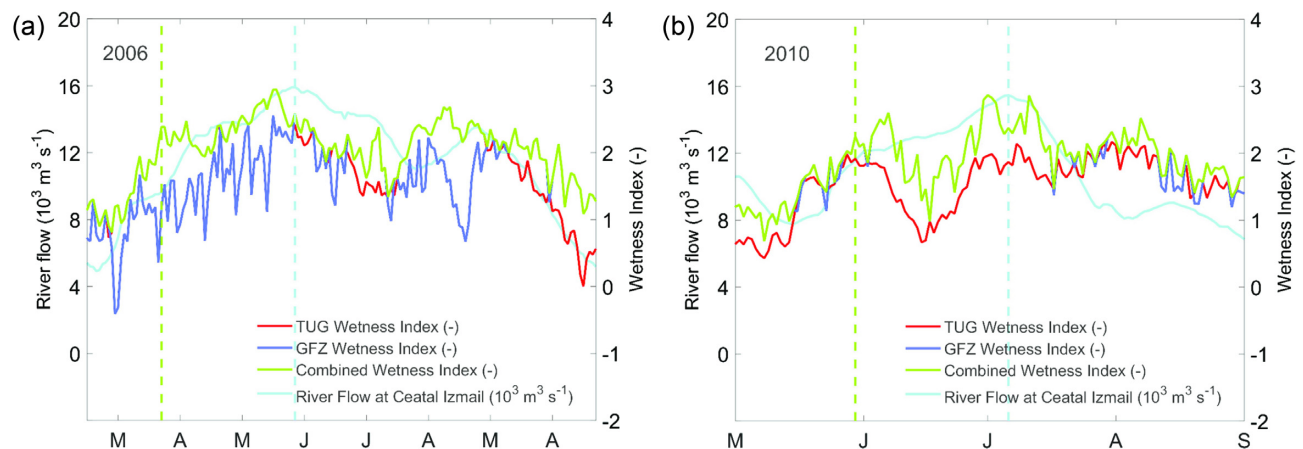

Figure 12. Basin-average gravity-derived WIs for the Danube basin for the 2006 (left-hand panel) and the 2010 (right-hand panel) flood together with discharge at the basin outlet, gauging station Ceatal Izmail. The vertical dashed lines indicate time of peak flow (cyan) and early flood warning (green) based on WI exceeding a threshold value of 2.

times, possibly indicating a different flood triggering mechanism with less water storage accumulation. A low of the wetness index reflects dry conditions during the 2003 and 2015 European heat waves. A gradual increase of the WI from 2003 to 2006 can be an indication of the persistence of low water storage as a consequence

of the drought event, and a reason why the floods in 2004 and 2005 are not captured by the gravity-based index.

Fig. 13 shows maps of total water storage anomalies and of the WIs for the Danube basin on 2006 April 26 when flow peaks at Ceatal Izmail station at the basin outlet. Increased gravity TWSA
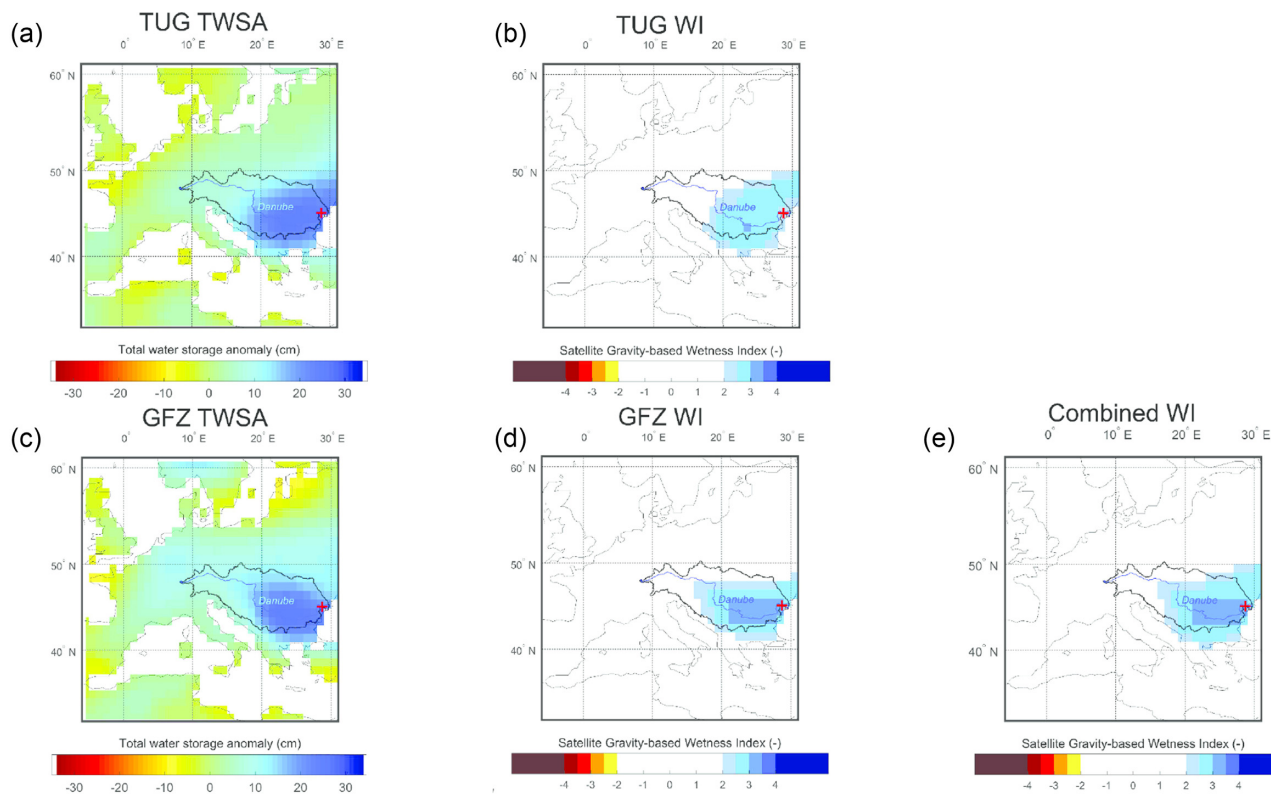
Figure 13. Daily gravity-based total water storage anomalies (TWSA) and gravity-based Wetness Indices (WI) for the Danube basin for 2006 April 26 based on TUG gravity solution (a, b), GFZ gravity solution (c,d) as well as the combined WI (e). The red cross indicates the location of the gauging station Ceatal Izmail.

values (dark blue) in both gravity solutions are reflected in elevated WI values, in particular in the lower parts of the river basin, with a spatially focused pattern of high WI by the GFZ gravity solution along the downstream reaches of the Danube where major flooding occurred. For the example of the Achleiten gauging station located at the German–Austrian border, the Upper Danube sub-basin size of just under $80\,000\,\mathrm{km}^2$ is at the limit of what is a physically detectable gravity signal by GRACE. In fact, lead-times prior to peak flow in the Upper Danube are critically reduced (2006) or even negative (2010). Thus, the potential of early flood warning by a detectable WI signal of elevated storage is markedly reduced for smaller upstream sub-basins.

6.2 Potential for early warning applications

Early warning by the wetness index presented here is expected to improve the programming and the efficient use of high resolution satellites that are used for disaster management activities such those carried out at DLR's Center for Satellite-Based Crisis Information (ZKI), being one of the main value adders of the International Charter (Voigt *et al.* 2007; Martinis *et al.* 2017). The International Charter 'Space and Major Disasters', which is an agreement of space agencies and satellite operators worldwide with the aim of providing a uniform system for the quick acquisition and delivery of EO data in case of disasters, is a major international activity in this respect (Voigt *et al.* 2016). Generally, the Charter mechanism is activated through authorized users. In some cases in the past, when user requests came in relatively late, satellite tasking could not be put into effect until the flood peak had already passed the area of interest. Here, for the example of the Danube flood in 2006,

we assess the value of early proactive satellite tasking based on external information from gravity-based wetness indicators before the actual activation of the Charter. As an example, Fig. 14 shows a map of flooded areas in the delta region of the river Danube in eastern Romania which was derived from MODIS (Moderate Resolution Imaging Spectroradiometer) data acquired on 2006 April 26. This corresponds to the time of the flood peak at Ceatal Izmail station at the outlet of the Danube basin (see Fig. 11). MODIS is a medium resolution optical satellite sensor with a spatial resolution of up to 250 m used for large-scale environmental monitoring (Masuoka *et al.* 1998). MODIS acquires images of the Earth's surface continuously every 1–2 d, provided that there are no clouds. Higher resolution satellites (particularly SAR satellites), which are more suitable for flood delineation even for cloudy conditions, need to be programmed prior to the flood peak in order to acquire up-to-date high resolution images of the flood affected regions to be used for disaster management activities. For the 2006 flood, the International Charter was activated for Romania on 2006 April 18 (Call No. 121, Table 4). The area affected in the Danube delta (see Fig. 14) was one of the two areas of interest (AOI) of the Charter call for which a number of rapid mapping products were produced based on the Charter satellite data, shown in Fig. 15, apart from the routinely available MODIS data acquired on 2006 April 26.

As an example, Fig. 15 shows four of the Charter satellites, for which acquisitions would have been possible for the Danube delta area (Fig. 14) based on the available overpasses during April 2006. This analysis has been carried out with the 'SaVoir Charter - Swath Acquisition Planner' V4.5.4.0 (©Taitus Software).

Taking into account the lead time of the gravity-based wetness index of 43 d prior to the flood peak at Ceatal Izmail station at the
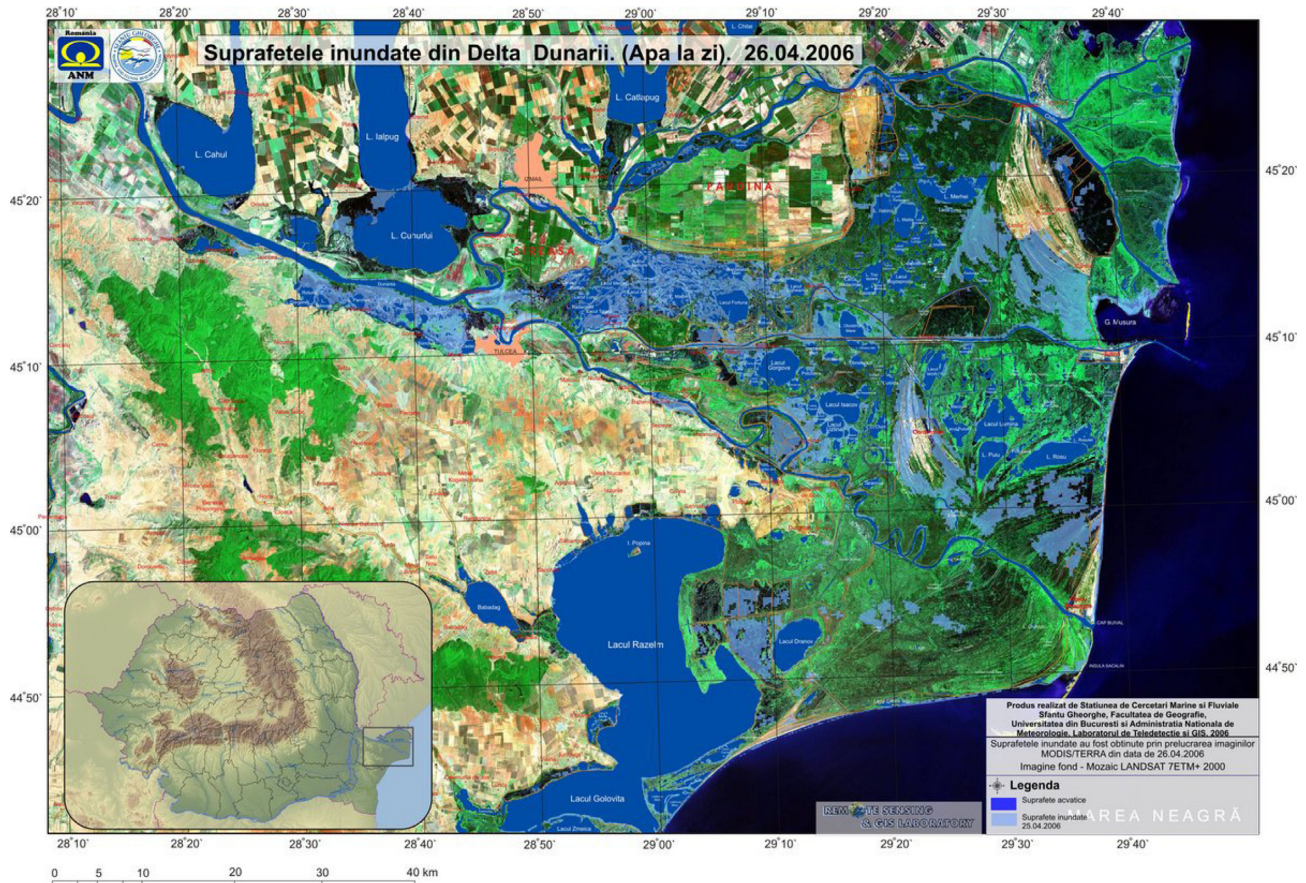
Figure 14. Map of flooded areas in the Danube delta based on MODIS data acquired on 2006 April 26 (source: https://disasterscharter.org/web/guest/-/flooding-in-romania).
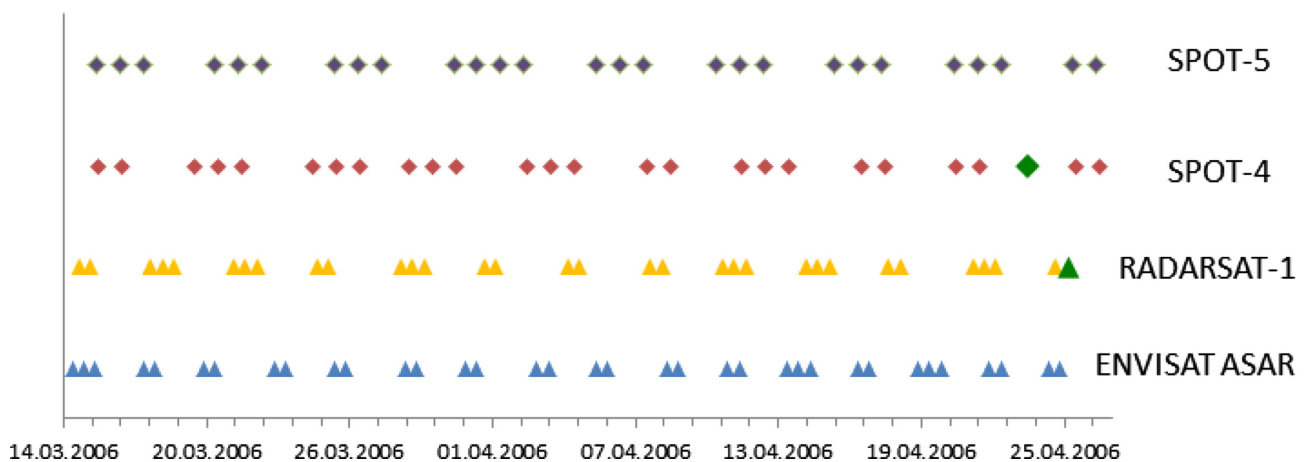

Figure 15. Possible overpasses and acquisitions of ENVISAT ASAR (wide swath mode with 150 m spatial resolution), Radarsat-1 (standard mode with 30 m spatial resolution), SPOT-4 (HRVIR sensor with 10 m spatial resolution) and SPOT-5 satellite (HRG sensor with 10 m spatial resolution) for the Danube delta region shown in Fig. 14. Acquisitions that have been realized during Charter Call 121 are marked with dark green symbols.

outlet of the Danube basin (see Fig. 12), a large number of additional satellite overpasses (35 for ENVISAT-ASAR, 32 for Radarsat-1, 26 for SPOT-4 and 27 for SPOT-5) would have been possible to acquire data for flood monitoring and emergency mapping if the wetness indices were available at that time. For the Danube flood 2006 the Charter was activated four times (Czech Republic/Slovakia: April 1; Austria: April 7; Hungary: April 14; Romania: April 18). The WI Early flood warning time stamp of the Upper Danube was 2006

March 13. Regarding the time when the Charter was first activated for the Danube flood on April 1 for the Czech Republic and Slovakia being the point in time when it was considered as a major disaster, an early flood warning lead time of 18 d can be determined in this case.

Requirements expressed by the users of satellite rapid mapping products focus on timely and high frequency flood monitoring from the onset of a flood event with special focus on mapping the flood

extent at peak level until water levels have receded to near normal stages. Based on the example of the Danube flood 2006 it could be demonstrated that gravity-based early-warning indicators for total water storage anomalies can improve the programming and the efficient use of EO satellites for rapid flood mapping tremendously. For the case of widespread flooding along the Danube in southern Romania after a dam break close to the village of Bistret on 2006 April 17 (not shown in detail here), proactive early satellite tasking would have offered the possibility to have satellite data available for disaster response teams a few hours after the dam break instead of a few days.

7 SUMMARY

The European GRACE ACs have joined forces to establish the European Gravity Service for Improved Emergency Management (EGSIEM) initiative. During the European Commission backed funding phase of 2015–2017, three prototype services were set up: (1) a scientific combination service, (2) an NRT service, and (3) a hydrological/early warning service. With the scientific combination service EGSIEM aimed to pave the way to a long-awaited standardization in the gravity field community. For a demonstration period of 2 yr normal equations of monthly GRACE gravity fields in terms of spherical harmonics were generated in the SINEX format by four ACs (AIUB, TUG, GFZ, CNES) by adopting different approaches but agreed upon processing standards. The resulting SINEX files were generated without regularizations and combined on the normal equation level to derive one consolidated monthly gravity field solution with significantly increased quality, robustness and reliability. With the end of the EGSIEM project in 2017 December, the scientific combination service is currently being extended to also include non-European ACs, to extend the time-series of combined monthly gravity fields covering the entire GRACE time period, and to be prepared for the upcoming release of GRACE-FO data. The service will be continued as the International Combination Service for Time-variable Gravity Fields (COST-G). COST-G will be officially launched as the product centre for time-variable gravity fields of IAG's International Gravity Field Service (IGFS) in 2019 July at the 27th General Assembly of the International Union of Geodesy and Geophysics (IUGG).

Within the NRT service, EGSIEM generated for the first time daily gravity field solutions in NRT using two different approaches at the ACs TUG and GFZ. The performance of the daily gravity solutions was tested using historical hydrological extreme events and relative intercomparisons between the two generated NRT time-series. An excellent agreement of the two solutions was found for these historical flood events, which was the proof-of-concept of this service. The operational test run took place from 2017 April 1 until June 29 but the deteriorating health of GRACE-B posed a serious challenge to the data processing. In terms of difference RMS over the continents, the two solutions differed approximately 2.8 cm during the operational test run, which is an increase of about 30 per cent compared to a similar three month time span in the offline test for 2008. Thus, the instrument performance was found to be the limiting factor in the quality of the gravity field solutions but we found no limiting factor in the procedure and workflow of the NRT service. The test can therefore be considered a success and the service is prepared for the soon to be released GRACE-FO data.

Within the hydrological service a wetness index was developed indicating departure of the GRACE-derived total water storage anomaly from a mean seasonal cycle (after removing the long-term trend). A retrospective analysis of both daily gravity field solutions showed increased values of the wetness index for the flood events in the Danube basin in 2002, 2006 and 2010. Of particular relevance with respect to early flood warning is the build-up of basin-wide water storage over several weeks prior to the larger flood events of 2006 and 2010. Elevated wetness indices of about two were registered with a lead-time of more than 6 and 5 weeks before the river peak flow at the basin outlet for the 2006 and 2010 floods, respectively, significantly exceeding the traveltime of flood waves from the upstream to the downstream parts of the basin. The gravity-based wetness index of the hydrological service has been incorporated into existing mapping and alerting systems for testing purposes. In particular, it has been included as a data layer into the European Commission's Copernicus Global Flood Awareness System (GloFAS) platform. At DLR/ZKI, an interactive web client has been developed to visualize the wetness index together with other DLR/ZKI data sources such as with results from DLR's operational Sentinel-1 (Twele *et al.* 2016) and TerraSAR-X Flood Services (Martinis *et al.* 2015). Being incorporated into the operational ZKI workflow the daily global gravity-based wetness index may serve as one of the triggers for an early and improved satellite tasking that offers high resolution (e.g. TerraSAR-X) acquisition planning for supporting disaster response and disaster management.

REFERENCES

Altamimi, Z., Collilieux, X. & Métivier, L., 2011. ITRF2008: an improved solution of the international terrestrial reference frame, *J. Geod.,* **85**(8), 457–473.

Altamimi, Z., Collilieux, X. & Métivier, L., 2016. ITRF2014: a new release of the International Terrestrial Reference Frame modeling nonlinear station motions, *J. Geophys Res.,* **121,** 6109–6131.

Argus, D., Peltier, W.R., Drummond, R. & Moore, A.W., 2014. The Antarctica component of postglacial rebound model ICE-6G_C(VM5a) based on GPS positioning, exposure age dating of ice thicknesses, and relative sea level histories, *Geophys J. Int.,* **198**(1), 537–563.

Arnold, D. *et al.*, 2015. CODE's new solar radiation pressure model for GNSS orbit determination, *J. Geod,* **89**(8), 775–791.

Bettadpur, S., 2012. CSR level-2 processing standards document for level-2 product release 0005, *GRACE,* 327–742.

Beutler, G., Jäggi, A., Mervart, L. & Meyer, U., 2010. The celestial mechanics approach: application to data of the GRACE mission, *J. Geod.,* **84**(11), 661–681.

Bianco, G., Devoti, R., Fermi, M., Luceri, V., Rutigliano, P. & Sciarretta, C., 1998. Estimation of low degree geopotential coefficients using SLR data, *Planet Space Sci.,* **46**(11-12), 1633–1638.

Bock, H., Dach, R., Jäggi, A. & Beutler, G., 2009. High-rate GPS clock corrections from CODE: support of 1 Hz applications, *J. Geod.,* **83**(11), 1083–1094.

Bock, Y. & Webb, F., 2012. MEaSUREs Solid Earth Science ESDR System. Available at: ftp://garner.ucsd.edu/pub/timeseries/measures/ats/Global/, accessed on June 6, 2019.

Brakenridge, G.R., 2016. Global Active Archive of Large Flood Events, Dartmouth Flood Observatory, University of Colorado. Available at: http://floodobservatory.colorado.edu/Archives/index.html (accessed on Nov 11, 2016).

Briggs, R., Pollard, D. & Tarasov, L., 2014. A data constrained large ensemble analysis of Antarctic evolution since the Eemian, *Quat. Sci. Rev.,* **103**(1), 91–115.

Bruinsma, S., Lemoine, J.-M., Biancale, R. & Valès, N., 2010. CNES/GRGS 10-day gravity field models (release 2) and their evaluation, *Adv. Space Res.,* **45,** 587–601.

Carrere, L., Lyard, F., Cancet, M., Guillot, A. & Picot, N., 2016. *FES 2014, a new tidal model – Validation results and perspectives for improvements, ESA Living Planet Conference, Prague, 2016*.

Cesare, S. & Sechi, G., 2013. Next Generation Gravity Mission, in *Distributed Space Missions for Earth System Monitoring,* pp. 575–598, ed., D'Errico, M., Springer.

Cheng, M., Shum, C. & Tapley, B., 1997. Determination of long-term changes in the Earth's gravity field from satellite laser ranging observations, *J. geophys. Res.,* **102**(B10), 22 377–22 390.

Chen, Q., Poropat, L., Zhang, L., Dobslaw, H., Weigelt, M. & van Dam, T., 2018. Validation of the EGSIEM GRACE Gravity Fields Using GNSS Coordinate Timeseries and In-Situ Ocean Bottom Pressure Records, *Remote Sens.*, **10**(12), 1976, doi:10.3390/rs10121976.

Dach, R., Schaer, S., Arnold, D., Prange, L., Sidorov, D., Sušnik, A., Villiger, A. & Jäggi, A., 2017. *CODE rapid product series for the IGS*. Published by Astronomical Institute, University of Bern. Available at: http://www.aiub.unibe.ch/download/CODE, doi:10.7892/boris.75854.1, accessed on June 6, 2019.

Dach, R. *et al.*, 2009. GNSS processing at CODE: status report, *J. Geod.,* **83**(3-4), 353–366.

Dahle, C., Flechtner, F., Gruber, C., König, D., König, R., Michalak, G. & Neumayer, K.H., 2012. GFZ GRACE Level-2 Processing Standards Document for Level-2 Product Release 0005. Scientific Technical Report STR12/02 - Data, Revised Edition, January 2013, Potsdam, doi:10.2312/GFZ.b103-1202-25.

Dahle, C., Flechtner, F., König, R., Michalak, G., Neumayer, K.-H., Gruber, C. & König, D., 2014. GFZ RL05: An Improved Time-Series of Monthly GRACE Gravity Field Solutions, in *Observation of the System Earth from Space - CHAMP, GRACE, GOCE and future missions,* pp. 29–39, eds Flechtner, F., Sneeuw, N. & Schuh, W.-D., Springer.

Davis, J.L., Elosegui, P., Mitrovica, J.X. & Tamisea, M.E., 2004. Climate-driven deformation of the solid Earth from GRACE and GPS, *Geophys. Res. Lett.,* **31**, L24605, doi:10.1029/2004GL021435.

Dobslaw, H., 2017. A new high-resolution model of non-tidal atmosphere and ocean mass variability for de-aliasing of satellite gravity observations: AOD1B RL06, *Geophys. J. Int.,* **211**(1), 263–269.

Dobslaw, H., Bergmann-Wolf, I., Dill, R., Forootan, E., Klemann, V., Kusche, J. & Sasgen, I., 2015. The updated ESA Earth System Model for future gravity mission simulation studies, *J. Geod.,* **89**(5), 505–513.

Dow, J.M., Neilan, R.E. & Rizos, C., 2009. The International GNSS Service in a changing landscape of Global Navigation Satellite Systems, *J. Geod.,* **83**(3), 191–198.

Drinkwater, M., Haagmans, R., Muzi, D., Popescu, A., Floberghagen, R., Kern, M. & Fehringer, M., 2006. The GOCE gravity mission: ESA's first core explorer, in *3rd GOCE User Workshop,* pp. 1–7, eds Frascati, Italy, ESA SP-627.

Döll, P., Kaspar, F. & Lehner, B., 2003. A global hydrological model for deriving water availability indicators: model tuning and validation, *J. Hydrol.,* **270**(1-2), 105–134.

Ellmer, M. & Mayer-Gürr, T., 2017. High precision dynamic orbit integration for spaceborne gravimetry in view of GRACE Follow-on, *Adv. Space Res.,* **70**(1), 1–13.

Emerton, R.E. *et al.*, 2016. Continental and global scale flood forecasting systems, *WIREs Water,* **3,** 391–418.

European Gravity Service for Improved Emergency Management (EGSIEM). Processing Standards, Models, EGSIEM-D2.1, Issue 1.0, 2015.

Flechtner, F., Kvas, A., Gruber, C., Mayer-Gürr, T., Güntner, A., Gouweleeuw, B. & Zwenzner, H., 2017. EGSIEM's Near Realtime Mass Transport Products For Monitoring Of Hydrological Extreme Events, Proceedings of the GRACE Science Team Meeting, Austin, Texas, USA, 12.10.2017, presentation available at http://www2.csr.utexas.edu/grace/GSTM/.

Flechtner, F., Morton, P., Watkins, M. & Webb, F., 2013. Status of the GRACE follow-on mission, in *Gravity, Geoid and Height Systems. IAG Symposia,* pp. 117–121, ed. Marti, U., IAG.

Flechtner, F., Neumayer, K.-H., Dahle, C., Dobslaw, H., Fagiolini, E., Raimondo, J.-C. & Güntner, A., 2016. What Can be Expected from the GRACE-FO Laser Ranging Interferometer for Earth Science Applications, *Surv. Geophys.,* **37**(2), 453–470.

Fritsche, M., 2014. Homogeneous reprocessing of GPS, GLONASS and SLR observations, *J. Geod.,* **88**(7), 625–642.

Gouweleeuw, B.T., Kvas, A., Gruber, C., Gain, A.K., Mayer-Gürr, T., Flechtner, F. & Güntner, A., 2018. Daily GRACE gravity field solutions track major flood events in the Ganges-Brahmaputra Delta, *Hydrol. Earth Syst. Sci.,* **22**, 2867–2880.

Gruber, C. & Gouweleeuw, B., 2019. Short latency monitoring of continental, ocean- and atmospheric mass variations using GRACE inter-satellite accelerations, *Geophys J. Int.,* **217**(1), 714–728.

Hughes, A.L.C., Gyllencreutz, R., Lohne, O.S., Mangerud, J. & Svendsen, J.I., 2015. The last Eurasian ice sheets - a chronological database and time-slice reconstruction, DATED-1, *Boreas,* **45**(1), 1–45.

Humphrey, V., Gudmundsson, L. & Seneviratne, S.I., 2016. Assessing global water storage variability from GRACE: trends, seasonal cycle, subseasonal anomalies and extremes, *Surv. Geophys.,* **37**(2), 357–395.

ICPDR, 2007. The analysis of the Danube, floods., 2006, ICDPR, report, Vienna, Austria.

ICPDR, 2012. 2010 Floods in the Danube river basin, brief overview of key events and lessons learned, ICDPR report, Vienna, Austria.

Jean, Y., Meyer, U. & Jäggi, A., 2018. Combination of GRACE monthly gravity field solutions from different processing strategies, *J. Geod.,* **92**(11), 1313–1328.

Kim, J., 2000. Simulation study of a low-low satellite-to-satellite tracking mission, Technical Report, University of Texas at Austin, TX, USA.

Klinger, B. & Mayer-Gürr, T., 2014. Combination of GRACE star camera and angular acceleration data: impact on monthly gravity field models. GRACE Science Team Meeting 2014, Potsdam

Klinger, B. & Mayer-Gürr, T., 2016. The role of accelerometer data calibration within GRACE gravity field recovery: Results from ITSG-Grace2016, *Adv. Space Res.,* **58**(9), 1597–1609.

Koch, K.R., 2007. *Introduction to Bayesian Statistics, Second, updated and enlarged Edition,* Springer.

Kurtenbach, E., Eicker, A., Mayer-Gürr, T., Holschneider, M., Hayn, M., Fuhrmann, M & Kusche, J., 2012. Improved daily GRACE gravity field solutions using a Kalman smoother, *J. Geodyn.,* **59-60,** 39–48.

Kusche, J., Schmidt, R., Petrovic, S. & Rietbroek, R., 2009. Decorrelated GRACE time-variable gravity solutions by GFZ, and their validation using a hydrological model, *J. Geod.*, **83**(10), 903–913.

Lambeck, K., Rouby, H., Purcell, A., Sun, Y. & Sambridge, M., 2014. Sea level and global ice volumes from the Last Glacial Maximum to the Holocene, *Proc. Natl. Acad. Sci. U S A,* **111**(43), 15 296–15 303.

Lecavalier, B.S., 2014. A model of Greenland ice sheet deglaciation constrained by observations of relative sea level and ice extent, *Quat Sci. Rev.,* **102**, 54–84.

Lemoine, F.G. *et al.*, 1997. The development of the NASA GSFC and NIMA joint geopotential model, in *IAG Symposia: Gravity, Geoid and Marine Geodesy,* pp. 461–469, eds Segawa, J., Fujimoto, H. & Okubo, S., Springer.

Loomis, B., Nerem, S. & Lutcke, S.B., 2012. Simulation study of a follow-on gravity mission to GRACE, *J. Geod.,* **86**(5), 319–335.

Martinis, S., Kersten, J. & Twele, A., 2015. A fully automated TerraSAR-X based flood service, *ISPRS J. Photogram. Remote Sens.,* **104,** 203–212.

Martinis, S., Twele, A., Plank, S., Zwenzner, H., Danzeglocke, J., Strunz, G., Lüttenberg, H.-P. & Dech, S., 2017. The International 'Charter Space and Major Disasters': DLR's contributions to emergency response worldwide, *J. Photogram. Remote Sens. Geoinform. Sci.,* **85,** 317–325.

Masuoka, E., Fleig, A., Wolfe, R.E. & Patt, F., 1998. Key Characteristics of MODIS Data Products, *IEEE T. Geosci. Remote,* **36**(4), 1313–1323.

Mayer-Gürr, T., Behzadpour, S., Ellmer, M., Kvas, A., Klinger, B. & Zehentner, N., 2016. ITSG-Grace2016 - Monthly and daily gravity field solutions from GRACE, *GFZ Data Services,* doi:10.5880/icgem.2016.007.

Mayer-Gürr, T., Eicker, A., Kurtenbach, E. & Ilk, K.H., 2010. ITG-GRACE: Global static and temporal gravity field models from GRACE data, in System Earth via Geodetic-Geophysical Space Techniques, edsFlechtner *et al.*, pp. 159–168, Springer.

Meyer, U., Jean, Y. & Jäggi, A., 2018. Combination of GRACE monthly gravity fields on normal equation level, *Under review*.

Meyer, U., Jäggi, A., Beutler, G. & Bock, H., 2015. The impact of common versus separate estimation of orbit parameters on GRACE gravity field solutions, *J. Geod.*, **89**(7), 685–696.

Meyer, U., Jäggi, A., Jean, Y. & Beutler, G., 2016. AIUB-RL02: an improved time series of monthly gravity fields from GRACE data, *Geophys J. Int.,* **205**(2), 1196–1207.

Nordman, M., Milne, G. & Tarasov, L., 2015. Reappraisal of the Angerman River decay time estimate and its application to determine uncertainty in Earth viscosity structure, *Geophys. J. Int.,* **201,** 811–822.

Pail, R. *et al.* 2015. Science and user needs for observing global mass transport to understand global change and to benefit society, *Surv. Geophys.,* **36**(6), 743–772.

Penna, N.T., King, M.A. & Stewart, M.P., 2007. GPS height time series: short-period origins of spurious long-period signals. *J. Geophys. Res.,* **112,** B02402, doi:10.1029/2005JB004047.

Petit, G. & Luzum, B., 2010. IERS Conventions 2010. IERS Technical note no.36. Bundesamt für Kartographie und Geodäsie, Frankfurt am Main, Germany.

Reager, J.T. & Famiglietti, J.S., 2009. Global terrestrial water storage capacity and flood potential using GRACE, *Geophys. Res. Lett.,* **36,** L23402, doi:10.1029/2009GL040826.

Reager, J.T., Thomas, B.F. & Famiglietti, J.S., 2014. River basin flood potential inferred using GRACE gravity observations at several months lead time. *Nat. Geosci.,* **7**(8), 589–593.

Rebischung, P., Zuheir, A., Jim, R. & Garayt, B., 2016. The IGS contribution to ITRF2014, *J. Geod.,* **90**(7), 611–630.

Reigber, C., Lühr, H. & Schwintzer, P., 1998. Status of the CHAMP Mission, in *Towards an Integrated Global Geodetic Observing System (IGGOS),* pp. 63–65, eds Rummel, R., Drewes, H., Bosch, W. & Hornik, H., Springer.

Root, B., Tarasov, L. & van der Wal, W., 2015. GRACE gravity observations constrain Weichselian ice thickness in the Barents Sea, *Geophys Res. Lett.,* **42,** 3313–3320.

Sakumura, C., Bettadpur, S. & Bruinsma, S., 2014. Ensemble prediction and intercomparison analysis of GRACE time-variable gravity field models, *Geophys Res. Lett.,* **41,** 1389–1397.

Shako, R. *et al.*, 2014. EIGEN-6C: A High-Resolution Global Gravity Combination Model Including GOCE Data, in *Observation of the System Earth from Space - CHAMP, GRACE, GOCE and future missions, GEOTECHNOLOGIEN Science Report No. 20,* pp. 155–161, eds Flechtner, F., Sneeuw, N. & Schuh, W.-D., Springer.

Sośnica, K., Jäggi, A., Meyer, U., Thaller, D., Beutler, G., Arnold, D. & Dach, R., 2015. Time variable Earth's gravity field from SLR satellites, *J. Geod.,* **89**(10), 1–16.

Steffen, H. *et al.*, 2017. Task 3.8 - GIA (correction) for hydrology Status June 2017, Presentation given at EGSIEM General Assembly 8-9 June 2017, DLR Oberphaffenhofen, Germany. Available at : http://egsiem.eu/images/static/PM_Oberpf_June2017/Annex10_WP3_GIA_Correction_Hydrology.pdf (last visited 2018/02/21).

Steigenberger, P., Rothacher, M., Dietrich, R., Fritsche, M., Rülke, A. & Vey, S., 2006. Reprocessing if a global GPS network, *J. geophys Res.,* **111,** B05402, doi:10.1029/2005JB003747.

Tapley, B.D., Bettadpur, S., Ries, J.C., Thompson, P.F. & Watkins, M., 2004. GRACE measurements of mass variability in the Earth system, *Science,* **305**(5683), 503–505.

Tapley, B.D. *et al.*, 2019. Contributions of GRACE to understanding climate change, *Nat. Clim. Change,* **9,** 358–369.

Tarasov, L., Dyke, A.S., Neal, R.M. & Peltier, W.R., 2012. A data-calibrated distribution of deglacial chronologies for the North American ice complex from glaciological modelling, *Earth planet. Sci. Lett.,* **315-316,** 30–40.

Tesmer, V., Steigenberger, P., van Dam, T. & Mayer-Gürr, T., 2011. Vertical deformations from homogeneously processed GRACE and global GPS long-term series, *J. Geod.,* **85**(5), 291–310.

Thomas, A.C., Reager, J.T., Famiglietti, J.S. & Rodell, M., 2014. A GRACE-based water storage deficit approach for hydrological drought characterization, *Geophys. Res. Lett.,* **41,** 1537–1545, doi:10.1002/2014GL059323.

Twele, A., Cao, W., Plank, S. & Martinis, S., 2016. Sentinel-1 based flood mapping: a fully automated processing chain, *Int. J. Remote Sens.,* **27,** 2990–3004.

van Dam, T., Wahr, J. & Lavallée, D., 2007. A comparison of annual vertical crustal displacements from GPS and Gravity Recovery and Climate Experiment (GRACE) over Europe, *J. geophys. Res.,* **112,** B03404, doi:10.1029/2006JB004335

Voigt, S., Kemper, T., Riedlinger, T., Kiefl, R., Scholte, K. & Mehl, H., 2007. Satellite image analysis for disaster and crisis-management support, *IEEE Trans. Geosci. Remote Sens.,* **45**(6), 1520–1528.

Voigt, S. *et al.*, 2016. Global trends in satellite-based emergency mapping, *Science,* **353**(6296), 247–252.

Watkins, M. & Yuan, D.N., 2012. JPL Level-2 Processing Standards Document, For Level-2 Product Release 05.

Wouters, B., Bonin, J.A., Chambers, D.P., Riva, R.E.M. & Wahr, J., 2014. GRACE, time-varying, gravity., Earth system dynamics and climate change, *Rep. Prog. Phys.,* **77,** 116801, doi:10.1088/0034-4885/77/11/116801.

Zumberge, J.F., Heflin, M.B., Jefferson, D.C., Watkins, M.M. & Webb, F.H., 1997. Precise point positioning for the efficient and robust analysis of GPS data from large networks, *J. geophys. Res.,* **102**(B3), 5005–5017.